Evidence from polymict ureilite meteorites for a single "rubble-pile" ureilite parent asteroid gardened by several distinct impactors

Hilary Downes[1*], David W. Mittlefehldt[2], Noriko T. Kita[3], John W. Valley[3]

[1] School of Earth Sciences, Birkbeck, University of London, Malet Street, London WC1E 7HX, UK; Also at: Lunar and Planetary Institute, 3600 Bay Area Boulevard, Houston, TX 77058, USA.

[2] mail code KR, NASA/Johnson Space Center, Houston, TX 77058, USA.

[3] Department of Geology and Geophysics, University of Wisconsin-Madison, 1215 W. Dayton St., Madison, WI 53706, USA

Abstract

Ureilites are ultramafic achondrite meteorites that have experienced igneous processing whilst retaining heterogeneity in mg# and oxygen isotope ratios. Polymict ureilites represent material derived from the surface of the ureilite parent asteroid(s). Electron microprobe analysis of more than 500 olivine and pyroxene clasts in six polymict ureilites reveals that they cover a statistically identical range of compositions to that shown by all known monomict ureilites. This is considered to be convincing evidence for derivation from a single parent asteroid. Many of the polymict ureilites also contain clasts that have identical compositions to the anomalously high Mn/Mg olivines and pyroxenes from the Hughes 009 monomict ureilite (here termed the "Hughes cluster"). Four of the six samples also contain distinctive ferroan lithic clasts that have been derived from oxidized impactors. The presence of several common distinctive lithologies within the polymict ureilites is additional evidence that the ureilites were derived from a single parent asteroid. Olivine in a large lithic clast of augite-bearing ureilitic has an mg# of 97, extending the compositional range of known ureilite material.

In situ oxygen three isotope analyses were carried out on individual ureilite minerals and lithic clasts from two polymict ureilites, using a new generation large radius secondary ion mass

spectrometer (SIMS) IMS 1280 with precision of typically better than 0.2-0.4 ‰ (2SD) which is improved by a factor of 5-10 in comparison to earlier SIMS studies. The oxygen isotope ratios of most ureilitic clasts fall on a narrow trend directly along the CCAM line, covering the observed range of data for monomict ureilites, and show a good anti-correlation with mg# of the analysed phases. Our SIMS technique with extraordinary capabilities of measuring individual sub-mm sized clasts with high precision was also applied to distinguish clasts from ureilitic origin to others. One ferroan lithic clast was identified as being an R-chondrite (($\Delta^{17}O$=3.4±0.2‰), the first occurrence in any polymict ureilite, while a second ferroan clast is unlike any known meteorite. The SIMS data identify an exotic enstatite grain as being derived from an enstatite chondrite or aubrite, and another pyroxene grain with $\Delta^{17}O$ of -0.4±0.2 ‰ as being unique material unrelated to any known meteorite type.

Our study confirms that ureilitic olivine clasts with mg#s < 85 are much more common than those with mg# > 85, which also show more variable Mn contents, including the melt-inclusion-bearing "Hughes cluster" ureilites. We interpret this to indicate that the parent ureilite asteroid was disrupted by a major impact at a time when melt was still present in regions with a bulk mg# > 85, giving rise to the two types of ureilites: common ferroan ones that were already residual after melting and less common magnesian ones that were still partially molten when disruption occurred, some of which are the result of interaction of melts with residual mantle during disruption. A single daughter asteroid re-accreted from the disrupted remnants of the mantle of the proto-ureilite asteroid, giving rise to a "rubble-pile" body that had material of a wide variety of compositions and shock states present on its surface. The analysed polymict ureilite meteorites represent regolith that subsequently formed on this asteroidal surface, including impact-derived material from at least six different meteoritic sources.

1. Introduction

Ureilites are the second largest group of achondrites. They are ultramafic meteorites composed of olivine, pyroxene, minor carbon, sulphide and metal (Goodrich, 1992; Mittlefehldt et al., 1998). Their high C content, roughly 3 wt% on average, distinguishes ureilites from other achondrites. Their silicate mineral compositions clearly indicate the loss of a basaltic component

through igneous processing, yet the suite is very heterogeneous in mg# (molar 100*(MgO/(MgO+FeO))). Another distinguishing characteristic of ureilites is their extremely heterogeneous O isotopic compositions that are very similar to those of the carbonaceous chondrite anhydrous mineral (CCAM) line (Clayton and Mayeda, 1988; 1996) which may reflect heterogeneity in their chondritic precursors. The mg# heterogeneity may also have been inherited from the nebula (Clayton and Mayeda, 1988; 1996) or may result from combined igneous and redox processes acting on the parent asteroid (Walker and Grove, 1993; Singletary and Grove, 2003; Goodrich et al. 2007). Despite numerous studies, the exact origin of ureilites remains unclear. The ~4.56Ga U-Pb age (Torigoye-Kita, 1995) and recent studies of short-lived chronometers (Goodrich et al., 2002; Kita et al., 2003; Lee et al., 2005) indicate that the parent asteroid of the ureilites differentiated very early in the history of the Solar System. Therefore, they contain important information about processes that formed small rocky planetesimals in the early Solar System.

Because of the compositional heterogeneity, it has not yet been established whether ureilites were derived from a single parent asteroid or from multiple parents (see Warren et al, 2006). Indeed, the wide variation in mineral mg#s and oxygen isotope ratios could be readily explained by an origin in multiple compositionally similar parent asteroids that had experienced a similar evolution. If all ureilites are derived from a single parent asteroid, then it cannot have achieved isotopic and chemical homogenization, i.e. it did not experience a magma-ocean stage. On the other hand, if they are derived from numerous different asteroids with different Fe/Mg ratios and oxygen isotope compositions, then the processes that formed them must have been extremely common in at least one region of the early Solar System. In either case they form a crucial test of our understanding of the formation of achondritic planetesimals from chondritic precursors. This study attempts to investigate the origin of ureilites and determine whether there are multiple parent asteroids for ureilites or just a single one, by examining the compositions of minerals in polymict ureilites (i.e. regolith breccias from asteroidal surfaces) and comparing them to monomict ureilites.

There are currently 203 recognized ureilites (census through Meteoritical Bulletin No. 91), which reduce to approximately 140 individual samples when pairing is taken into account. Most

ureilites are unbrecciated, the so-called monomict ureilites. The cores of silicate minerals in each monomict ureilite are homogeneous in cation composition. Thus, only a maximum of ~140 data points are available from these rocks to constrain the composition of the ureilite parent asteroid(s). However, there are 17 known brecciated ureilites, although some of these are paired. All brecciated ureilites except possibly one are polymict. The sole exception is Frontier Mountains (FRO) 93008 (and paired meteorites) which is considered by Goodrich et al. (2004) to be a dimict breccia. However Welten et al. (2006) pair it with 8 other ureilites based on major element compositions and cosmogenic nuclide contents, and describe it as polymict. Each thin-section of a polymict ureilite may contain hundreds of clasts of ureilitic material, and multiple thin-sections greatly increase the number of clasts available for analysis. Therefore the potential for studying the parent asteroid(s) of ureilites is much greater if polymict samples are analysed.

We have undertaken a detailed study of mineral compositions in polymict ureilite meteorites that provide information about the regolith of their parent asteroid(s). We have analysed over 500 mineral or lithic clasts from six polymict ureilites and FRO 93008. Our goals were to evaluate whether ureilites were derived from a single parent asteroid, to gain further understanding of the evolution of the parent asteroid, and to understand ureilite petrogenesis.

2. Analytical methods

2.1 Electron microbeam techniques.

The polymict ureilites were investigated petrographically by SEM, using back-scatter electron images. The electron microprobe analyses were done using the Cameca SX100 wavelength dispersive electron microprobe at NASA Johnson Space Center. An average was taken of three spots per grain. Analytical conditions were 20 kV, 40 nA, 1 μm beam for olivine and pyroxene. For olivine, counting times were 120 seconds for Ca, Cr and Mn, and 40 seconds for Mg, Si and Fe. For pyroxenes, counting times were 120 seconds for Mn, 100 seconds for Na, Al and Ca, 80 seconds for Ti, 60 seconds for Cr, and 20 seconds for Mg, Si and Fe. High and low background counts were each half the duration of the peak counts. A Mn garnet was used as the Mn

standard, Cr metal for that element, and kaersutite for all other elements. Data reduction was done using the Cameca PAP data reduction routine.

Up to one hundred individual silicate mineral clasts, and a much smaller number of lithic clasts, were selected from the polished sections of each sample. A wide range of clast and grain sizes was analysed. Other criteria for selection included a wide range of contrast in BSE images in an effort to obtain coverage of the variation in Fe contents in the clasts. Reported analyses were made only on the cores of mineral clasts, i.e. reduced rims were avoided. Representative results are given in Table 1 (olivine) and Table 2 (pyroxene).

2.2 Oxygen isotope measurements

In-situ oxygen three isotope analyses were carried out on two sections (Elephant Moraine (EET) 83309,51 and EET 87720,41) using a CAMECA IMS-1280 ion microprobe at the University of Wisconsin-Madison. The analytical conditions were modified from Kita et al. (2004), which used an IMS-1270 in multi-collection mode. In addition to a number of improvements to the IMS-1280 hardware and software, we used high primary Cs^+ ion intensities of 6 nA (~15 μm spot diameter) and obtained high secondary $^{16}O^-$ ion intensities of 5×10^9 cps (Kita et al., 2007). In these conditions, all three oxygen isotopes are measured using Faraday Cup detectors with sufficient S/N ratios. Detailed analytical parameters are described in the electronic annex EA-1. The instrumental mass fractionation factors of olivine and pyroxene are evaluated using terrestrial standard minerals with known $\delta^{18}O_{VSMOW}$ values. The typical external errors of repeated San Carlos olivine standard analyses on different spots of homogeneous standards were 0.3-0.4 ‰ (2SD) for $\delta^{18}O$, $\delta^{17}O$ and $\Delta^{17}O$ (= $\delta^{17}O - 0.52 \times \delta^{18}O$), which we consider to be the uncertainty of individual spot analyses (Table EA1).

3. Petrography of selected polymict samples

The polymict ureilite samples studied at JSC were obtained from numerous sources. Dar al Gani ureilites were purchased as small slices. The Elephant Moraine and Frontier Mountains samples were obtained as interior chips. These samples were made into polished thick sections at JSC for petrographic study and future laser ablation ICP-MS analyses. The North Haig sections were

154 provided by the Western Australia Museum, and C. Goodrich kindly loaned us two thin sections
155 of Nilpena. A new polished thick-section of FRO 93008 was provided by L. Folco.
156
157 Samples investigated include two from Antarctica (EET 83309, EET 87720), two from Australia
158 (North Haig, Nilpena) and two from Libya (Dar al Gani (DaG) 999, DaG 1000). Two sections
159 were investigated from EET 87720 (sections 13, 41), EET 83309 (sections 50, 51), North Haig
160 (A, B) and Nilpena (A, B), and one section from each of the DaG samples. In addition, a new
161 section of the Antarctic ureilite FRO 93008 has been investigated. A large number of ureilites
162 have been found in the Dar al Gani region, and many of these are polymict. Thus we consider
163 that the two polymict DaG meteorites we have investigated are most likely paired. We have also
164 done a cursory petrographic study of two other Libyan polymict ureilites, DaG 1023 and DaG
165 976, but the samples obtained proved to be single ureilite clasts.
166
167 Goodrich et al. (2004) provided a review of polymict ureilites, including all of the samples
168 examined in this study. EET 83309, EET 87720 and Nilpena contain solar-wind implanted gases,
169 indicating derivation from regolith (Rai et al., 2003). Warren and Kallemeyn (1989, 1992)
170 reported the bulk compositions of EET 83309 and EET 87720. Guan and Crozaz (2000, 2001)
171 reported electron microprobe and ion microprobe results for EET 87720 and EET 83309. Cohen
172 et al. (2004) presented electron microprobe analyses of melt-derived feldspathic clasts in DaG
173 164, DaG 165, DaG 319, DaG 665 and EET 83309. Ikeda et al. (2000, 2003) and Ikeda and Prinz
174 (2001) studied the compositional variation of mineral clasts in DaG 319, while Kita et al. (2004)
175 investigated their oxygen isotope compositions.
176
177 *3.1 Elephant Moraine samples*
178
179 Figure 1 shows the typical textures of the EET samples. Schwarz and Mason (1989) described
180 EET 87720 as a "cataclastic aggregate." It has a cosmic-ray exposure (CRE) age of 8.9 Ma (Rai
181 et al., 2003).Warren and Kallemeyn (1989) and Guan and Crozaz (2001) have shown that it
182 contains numerous ureilitic olivine and pigeonite clasts that have been shocked to different
183 extents, as well as rare exotic grains of albitic plagioclase, nearly pure forsterite and nearly pure
184 enstatite. The matrix also includes abundant carbon phases, sulphides, suessite (Si-bearing Fe,Ni

metal) and kamacite. There are a number of strongly zoned ureilitic olivines with Mg-rich rims spotted with Fe-metal. Several sections of this meteorite contain very large clasts (i.e. >1.5 cm) of shocked mosaicised ureilite, composed of olivine with interstitial pigeonite, set in a brecciated matrix dominated by fragments of ureilitic olivine and pyroxene. One section (,41) also contains a large (0.5 cm) clast of a coarse-grained lithology composed of ferroan olivine with subordinate sodic plagioclase, rare pyroxene and pyrrhotite (Fig.1).

EET 83309 was described by Mason (1986), Prinz et al. (1987) and Warren and Kallemeyn (1989). It has a CRE age of 46.8 Ma (Rai et al., 2003). Our sections of EET 83309 (Fig.1) are mostly formed of angular clasts of ureilitic olivine, pigeonite and rare augite, together with single large mineral clasts of enstatite, plagioclase (including some pure anorthite compositions) and a single grain of chromite. The matrix contains carbon, kamacite, suessite and troilite. Single grains of ureilite olivine are up to 1 mm in diameter, but most are much smaller. Both sections contain rock clasts at least 0.2 cm across, containing ferroan olivine with subordinate plagioclase, pyroxene, chromite and pyrrhotite (Fig.1). The different CRE ages of EET 83309 and EET 87520 demonstrate that they are not paired, in spite of some petrographic similarities between these two meteorites found only 15 km apart.

3.2 Australian samples

North Haig was found in western Australia and was initially described by Berkley et al. (1980) and Prinz et al. (1983). The possibility of it being paired with Nilpena was discussed by Prinz et al. (1986) but later discounted (Prinz et al., 1987). No CRE age is available for North Haig. Two sections of North Haig were obtained from the Museum of Western Australia (sample number 12809). Both are large thin-sections; section A is 0.7 x 0.6 cm and B is 1.3 x 0.7 cm. However, section A is composed of a single lithic clast. Section B is a typical polymict breccia, containing a wide variety of olivine and pyroxene clasts up to 2 mm in diameter, together with some plagioclase clasts and carbon phases. Nilpena is from South Australia and was described by Jaques and Fitzgerald (1982). It has a CRE age of 9.8 Ma (Rai et al., 2003). Two sections of Nilpena were analysed. Section A is 2 cm long by 6 mm wide, whereas section B has an area of approximately 1 cm^2. Both are coarse-grained polymict breccias containing a variety of angular

and rounded clasts of olivine, pigeonite and augite, together with abundant carbon phases, rare plagioclase and a few melt clasts. North Haig and Nilpena contain much less metal than do the Antarctic samples, possibly due to more extensive weathering.

3.3 Dar al Gani samples

Russell et al. (2003) have previously described DaG 999 and DaG 1000. Although no studies have been directed toward testing for a possible pairing relationship, these two stones were found within 1.4 km of each other. Furthermore, their positions were 0.7 km E and 1.8 km SE, respectively, of the location of the well-known polymict ureilite DaG 319, with which they are therefore probably paired. No CRE ages are available, but DaG 319 has a CRE age of 21.5 Ma. The section of DaG 999 covered an area of 2 x 2 cm. It is a coarse-grained carbon-bearing polymict ureilite that contains a large (0.5 cm diameter) clast of an augite-bearing ureilite lithology. A second large clast (1 cm diameter) is composed of olivine-pigeonite ureilite. DaG 999 also contains an exotic clast of a ferroan olivine lithology, and grains of pure anorthitic feldspar. The section of DaG 1000 investigated measured 1.5 x 1.5 cm. It contains abundant angular and rounded clasts of olivine, pigeonite and augite up to 0.5 cm in diameter, displaying various levels of shock, two non-indigenous clasts of a ferroan olivine lithology similar to those described in EET 87720, abundant carbon phases and several grains of plagioclase.

3.4 FRO 93008

The brecciated and possible polymict nature of the Frontier Mountains ureilites was first suggested by the petrological studies of Smith et al. (2000) and Fioretti and Goodrich (2001). Fioretti and Molin (1996) demonstrated that FRO 93008 and FRO 90054 are paired. More recently, Welten et al. (2006) showed from cosmogenic radionuclides that most of the FRO ureilites, including FRO 93008, are likely derived from a single fall. Smith et al. (2000) found three distinct olivine compositional populations among the six FRO ureilites they examined. This, plus the few exogenous clasts found along the contacts between major ureilite lithologies (see Fioretti and Goodrich, 2001; Goodrich et al., 2004), would favor a polymict designation, as advocated by Welten et al. (2006). Goodrich et al. (2004) noted that one of the olivine groups is

represented by mosaicized olivines, and suggested that these had their original compositions altered by the late shock event; they favored classification as dimict breccias for the paired FRO ureilites. Regardless, since the FRO breccia is composed of a few very large clasts, it may represent a more coarsely brecciated portion of its parent asteroid than the finer-grained regolith-derived polymict breccias. The latter represent the surface of the ureilite parent asteroid, while the FRO pairing group may represent a deeper portion of the breccia zone of the asteroid's outer reaches.

Our new section (04) is very similar to that described by Smith (2002) and is composed of two strongly contrasting lithologies: (a) a coarse-grained carbon-free magnesian augite-olivine-pigeonite rock and (b) a less magnesian olivine-pigeonite rock with strongly mosaicized olivine and abundant carbon. The difference between the carbon contents of the two lithologies is striking. Augite poikilitically encloses rounded olivine crystals in the augite-rich lithology in a texture similar to that described by Takeda et al. (1989) for Yamato (Y) 74130 and Meteorite Hills (META) 78008 where ellipsoidal pigeonite is enclosed by augite. However, it differs from the texture of Lewis Cliff (LEW) 88774 (Goodrich, 1999) and HaH 064 (Weber and Bischoff, 1998) in which augite is itself enclosed by orthopyroxene oikocrysts, and is clearly different from the texture of Hughes 009 in which equant augite crystals are in textural equilibrium with olivine and orthopyroxene (Goodrich et al., 2001). Melt inclusions strikingly similar to those in Hughes 009 are also present within olivines in the augite-bearing portion of FRO 93008.

4. Results

4.1 Olivine compositions

Olivine core compositions of 34 monomict ureilites were previously analyzed at JSC (Hudon and Mittlefehldt, data in EA-2) using the analytical protocols used in this study. Figure 2 shows that almost all olivines from these monomict samples fall on the previously established ureilite Fe/Mn vs. Fe/Mg trend and demonstrates that the electron microprobe data in this paper are compatible with those of Goodrich et al. (2004). Olivine core mg#s range from 76 (Grosvenor Mountains (GRO) 95575) to 95 (Allan Hills (ALH) 82130), thus covering the entire range of

known ureilite compositions. The monomict ureilitic olivines display narrow ranges of minor element contents (0.38-0.55 wt% MnO, 0.26-0.42 wt% CaO and 0.4-0.9 wt% Cr_2O_3) in agreement with previous studies (see Mittlefehldt et al., 1998). As already noted by Goodrich et al. (2004), several poikilitic-textured orthopyroxene-bearing EET samples (EET 87511, EET 87523, EET 87717, EET 96322, EET 96328 and EET 96262) are paired, all having mg#s of 84.9. Olivines from several augite-bearing Antarctic ureilites (EET 96314, EET 96331 and EET 96293) have identical olivine compositions (mg#s = 86.8) and textural features and must therefore be paired. However, they plot below the ureilite trend with slightly higher Mn/Mg values (Fig. 2) and are very similar in composition to those of olivines from the unusual augite-bearing monomict ureilite Hughes 009 (Goodrich et al., 2001). Olivines from monomict ureilites and olivine clasts in polymict ureilites plotting in this area will be referred to subsequently as the "Hughes cluster".

In addition, to demonstrate the reproducibility of the electron microprobe analyses and the homogeneity of individual ureilites, analyses of several olivines from the single ureilite clast that constitutes our sample of DaG 1023 are reported on Fig. 2. Figure 2 also compares our analyses of olivine from the heterogeneous ureilite FRO 93008 with the ureilite trend and confirms that two compositions of olivine (Fo87 and Fo78) are present. Olivine compositions from the poikilitic augite-olivine-pigeonite lithology in FRO 93008 fall precisely on the field for olivines from the "Hughes cluster".

More than 330 olivine clasts have been analysed from the six polymict samples. A selection of the data is presented in Table 1. The vast majority of olivine clasts in the polymict ureilites display very similar range of CaO and Cr_2O_3 contents to those in olivine in monomict ureilites. Olivines with compositions greatly outside these values are considered to be non-indigenous. Figure 3 shows the complete data set for olivines, including non-indigenous clasts, from all six samples plotted on the conventional Fe/Mg vs. Fe/Mn diagram (Mittlefehldt, 1986). All of the polymict ureilites contain a wide range of olivine compositions that fall on the ureilite trend, covering the entire compositional range of monomict ureilites. In addition DaG 999 and EET 87720 contain a few ureilitic olivine clasts whose compositions are identical to those found in Hughes 009, thus forming part of the "Hughes cluster". Olivines from the large olivine-augite-

309 pigeonite clast in DaG 999 are very highly magnesian (Fo97) but have 0.32 wt % CaO and 0.49
310 wt% Cr_2O_3, well within the normal range of monomict ureilitic olivines. The discovery of this
311 clast extends the range of compositions of ureilites to Fo97, beyond that of monomict ureilites
312 (for which the most Mg-rich is ALH82106 with Fo94).
313
314 Olivines from the ferroan olivine clasts in several polymict samples have a narrow range of
315 compositions (Fo59-65; Table 1) and clearly plot beyond the range of the ureilite trend (Fig. 3).
316 Their NiO contents are ca. 0.5 wt%, in contrast to ureilitic olivines which have <0.01 wt% NiO
317 (Goodrich et al., 1987), and their Cr contents (<0.08 wt% Cr_2O_3) are much lower than in ureilitic
318 olivines. No ferroan clasts were found in our section of FRO 93008, but Fioretti and Goodrich
319 (2001) and Smith (2002) reported the presence of clasts of low-Cr olivine of Fo62 composition
320 in the boundary between the two lithologies, which probably belong to the ferroan olivine group.
321
322 A few less abundant olivine clasts have much lower MnO contents, low Mn/Mg ratios and, in
323 some cases, low CaO and Cr_2O_3 contents. They plot above the ureilite trend (Fig. 3). According
324 to Jaques and Fitzgerald (1982) and Ikeda et al. (2000), they are probably derived from
325 chondritic impactors on the surface of the ureilite parent asteroid. Two other olivine clasts (grain
326 34 from North Haig section B and grain 103 from DaG 999) have higher Mn/Mg ratios than
327 normal ureilite olivines and lie off the array (Fig. 3). They have CaO and Cr_2O_3 concentrations
328 that are close to those of normal ureilitic olivines and resemble olivines in igneous melt-clasts
329 from polymict ureilites (Ikeda et al., 2000; Cohen et al., 2004).
330
331 Data for olivine clasts have been plotted on individual Fe/Mn vs. Fe/Mg diagrams for each
332 polymict ureilite (Fig. 4). Results from each sample show as wide a spread of compositions as all
333 monomict ureilites. Most of the data are in the Fe-rich range, similar to the distribution of
334 monomict ureilite suite (Mittlefehldt et al., 1998). Ureilitic olivine compositions in all polymict
335 ureilites start abruptly at Fe/Mg values of 0.36 (Fo74). There appears to be a compositional gap
336 between Fe/Mg = 0.16 and 0.19 (Fo84 and Fo86) in EET 87720, North Haig and DaG 1000. The
337 distributions of olivine compositions from all six polymict samples are generally similar, but not
338 identical (Fig. 4). Since they have different CRE age, the polymict ureilites were excavated

339 during several different impact events and the distributions may reflect different relative
340 contributions of "source regions" locally exposed on the parent asteroid(s).
341
342 Figure 5 presents a histogram of mg# in all ureilitic olivine clasts from the six polymict samples.
343 Care has been taken to remove examples of repeat analyses of the same clast (e.g., the large
344 mosaicised clast in EET 87720,13) and exotic clasts such as those derived from chondrites. The
345 distribution of compositions is broadly similar to that reported for monomict ureilites by
346 Goodrich et al. (2004), with a major peak at Fo78-79. However, a minor peak at Fo86-87 is
347 present in the polymict olivine data that does not coincide with the peaks seen in data from
348 individual monomict ureilites. The new data fill in the apparent gaps at Fo83 and Fo89 seen in
349 monomict samples (Mittlefehldt et al., 2005) and thus predict that monomict ureilites of these
350 compositions must exist but have not yet been found. The histogram derived from the
351 compositions of polymict clasts clearly confirms the observation of Ikeda et al. (2000) that there
352 is a much higher proportion of ureilitic olivines with mg# < 85 than those with mg# > 85. Note
353 that the two data sets are not rigorously comparable, however. The monomict data are a random
354 sampling of material being delivered to Earth from the ureilite parent asteroid, while some
355 degree of human selection has been used to acquire the polymict data set.
356
357 *4.2 Pyroxene compositions*
358
359 Pyroxenes from the 34 monomict ureilites analysed by Hudon and Mittlefehldt (data in EA-2)
360 are mainly pigeonites with subordinate orthopyroxenes and rare augite. They plot on a similar
361 Fe/Mn-Fe/Mg trend to that seen in ureilitic olivines. More than 180 pyroxene clasts from the
362 polymict ureilites have been analysed (representative analyses, Table 2), including some augite
363 clasts. Figure 6 shows that the wide range of Fe/Mn and Fe/Mg in polymict ureilitic pyroxenes is
364 similar to the range in the whole suite of monomict ureilites. In addition to the pyroxenes that fall
365 on the trend shown by monomict ureilites, polymict ureilites contain pyroxene clasts with low
366 Mn/Mg ratios that plot well above the ureilite trend and are probably derived from non-ureilitic
367 impactors. Several pyroxenes mainly from DaG 1000 and Nilpena have slightly high Mn/Mg
368 ratios, similar to that of pyroxenes in Hughes 009 (Fig. 6). Furthermore, numerous pyroxene
369 compositions form a sub-horizontal trend towards higher Fe/Mg ratios, with little change in

Fe/Mn ratio. This trend is identical to that shown by pyroxenes in igneous clasts of the "albitic lithology" analysed by Cohen et al. (2004) from various polymict ureilites (Fig. 6). Pyroxenes that show this trend are probably fragments of similar ureilitic igneous clasts. This igneous trend appears to intersect the main ureilite trend near to the composition of the "Hughes cluster" samples, some of which contain melt inclusions.

Mosaicised clasts mainly in EET 87720 contain pyroxenes with slightly lower Mn/Mg ratios than normal ureilitic pigeonites, i.e. they plot above the main ureilite trend. This may be a consequence of shock redistribution of minor elements because all these clasts are strongly shocked but this requires further investigation. Pigeonites and augites from the olivine-augite-pigeonite clast in DaG 999 are highly magnesian (mg#s = 97). Orthopyroxenes from the ferroan clasts tend to have mg#s in the range 68-70, but a few have lower mg#s, indicating a lack of mineral equilibration in these clasts. Chondritic enstatite pyroxenes with very high mg#s and very low Ca contents (<0.4 wt% CaO) occur in most of the polymict samples.

Figure 7 shows the Ca contents and mg#s of pyroxenes from monomict and polymict ureilites. In this study, augite has been found as very rare small rounded inclusions in olivine in monomict ureilite EET 87517 and as an abundant interstitial phase in the paired stones EET 96293, EET 96314 and EET 96331. Rare single mineral clasts of augite in DaG 1000, DaG 999, Nilpena, North Haig and EET 83309 cluster around the composition of augites from the "Hughes cluster" (Hughes 009, EET 96293, FRO 93008 etc). The highly magnesian augites from the large olivine-augite-pigeonite ureilite clast in DaG 999 resemble those from the most magnesian ureilite ALH 82106. The remaining augite clasts from EET 83309 and EET 87720 have mg#s < 75. With the exception of one that is located within a ferroan clast (mg# = 64), these clasts, as well as the pigeonites with mg#s < 75 found mainly in Nilpena, are probably derived from the breakup of igneous-textured clasts similar to those described by Cohen et al. (2004) and hence may represent some of the missing basalt melts of the ureilite parent asteroid. Exotic clasts of chondritic diopside were also found in North Haig and Nilpena.

4.3 Oxygen isotopic compositions

401 The oxygen isotope data on ureilitic and non-ureilitic clasts are shown in Table 3. Six ureilitic
402 clasts, 1 ferroan clast and 1 enstatite single grain were analysed in section EET 83309,51 and 20
403 ureilitic clasts and one large ferroan clast in section EET87720,41. Some of the larger clasts were
404 measured in more than one spot, though none of these clasts showed internal heterogeneity in
405 oxygen isotope ratios. The oxygen isotope compositions of individual clasts are shown in Figure
406 8 and $\Delta^{17}O$ values are plotted against mg# in Figure 9. Figure 8 shows that, although the ion
407 microprobe data have larger analytical errors than the earlier bulk analyses of much larger
408 samples, the in situ data obtained in this study plot tightly on the CCAM line defined by Clayton
409 and Mayeda (1996). Furthermore, most ureilitic clasts plot within the range of those of monomict
410 ureilite data (Clayton and Mayeda, 1996). However, one magnesian pigeonite single grain clast
411 (EET 83309, 51, Gr20) significantly deviates in oxygen isotopic compositions from the ureilitic
412 region. The $\Delta^{17}O$ of this clast (-0.4 ‰) is at the high end of the ureilite range, but it has a high
413 mg# (93.5) and deviates from the ureilitic trend in Fig. 9. It may be an exotic clast that was not
414 previously distinguished by its chemical composition.
415
416 One of the ureilitic olivine clasts analyzed in this study, EET87720, 41 Gr38, is characterized as
417 being part of the "Hughes cluster" from its Mn content (Table 1; Fig. 2). Data from this clast plot
418 on the CCAM line in Fig. 8, though the $\Delta^{17}O$ value of -1.2‰ is slightly off the mg#-$\Delta^{17}O$ trend
419 compared to other magnesian samples in Fig. 9. The oxygen isotopic compositions of this clast
420 are in good agreement with those of Hughes 009 (Clayton and Mayeda, 1996) within analytical
421 errors. Ikeda and Prinz (2001) studied carbon-free clasts in polymict ureilite DaG 319 that
422 resemble Hughes 009, their "type II ureilitic clasts". The oxygen isotope ratios of these clasts are
423 also consistent with that of Hughes 009 (Kita et al., 2004).
424
425 Two ferroan clasts plot in completely different locations on the 3-isotope diagram (Fig. 8); one
426 from EET83309, 51 plots in the region close to R-chondrites, but the other clast from EET87720,
427 41 plots very near to the Terrestrial Fractionation (TF) line and close to the brachinite region.
428 The single nearly pure enstatite clast (EET83309, 51 Gr1) also plots on the TF line, consistent
429 with being derived from an enstatite chondrite or aubrite.
430
431 **5. Discussion**

Our petrographic observations, and electron microprobe and O isotopic data on mineral and lithic clasts from polymict ureilites, coupled with literature data from monomict and polymict ureilites allow us to examine several issues regarding the origin of ureilites. Here we will primarily address (i) whether the ureilite suite was derived from more than one parent asteroid, (ii) the types of impactors that gardened ureilites to produce the polymict breccias, and (iii) whether there are distinct groupings of ureilites.

5.1 Ferroan clasts and exotic mineral grains

We have found exotic ferroan clasts in 4 of the 6 polymict ureilites analysed (DaG 999, DaG 1000, EET 83309 and EET 87720). Similar clasts have been reported from polymict ureilite DaG 319 by Ikeda et al (2000, 2003), who referred to them as "equilibrated chondrite clasts" and noted their similarity to R-chondrites. Cohen et al. (2004) described a "feldspathic olivine augite" clast C24 with an olivine composition of Fo63 from polymict ureilite DaG 164. This clast is probably an exotic ferroan clast like those described here. The presence of such clasts in all the DaG polymict ureilites is not surprising, given that they are probably paired. Single grains of Fo60 olivine have also been reported in FRO 93008 (Fioretti and Goodrich, 2001), FRO 90168 and FRO 90228 (Smith, 2002); these have most probably been derived from fragmentation of ferroan clasts.

The olivine compositions, the presence of chromite and pyrrhotite and the absence of metal suggest a similarity to R chondrites. However, the two ferroan clasts analysed have different oxygen isotope ratios (Table 3; Fig. 8). The ferroan clast from EET 83309,51 has oxygen isotope ratios that plot within the field for R chondrites. We conclude that this clast is indeed a fragment of an R chondrite. In contrast, the ferroan clast from EET 87720,41 has oxygen isotopic compositions that plot within uncertainty of the terrestrial fractionation line (Fig. 8). Ikeda et al. (2003) determined the oxygen isotopic composition of one ferroan clast (equilibrated chondrite clast β 22B) that is within the rather large error limits identical to the clast from EET 87720,41. This indicates that there are two distinct populations of ferroan clasts that must have been derived from different parent bodies.

463

464 The EET 87720,41 and DaG 319 β 22B ferroan clasts are unlike any known meteorites, but must
465 represent a parent asteroid with a similar oxidation state to that of R chondrites. Brachinites are
466 oxidized achondrites (e.g. Mittlefehldt et al., 2003), and the oxygen isotopic composition of the
467 EET 87720,41 ferroan clast is similar to those of brachinites (Clayton and Mayeda, 1996).
468 However, brachinites are not quite as oxidized as the ferroan clasts, as they have olivine mg#s in
469 the range 64-71 (Mittlefehldt et al., 2003). Furthermore brachinites contain calcic pyroxenes that
470 are not present in the ferroan clast in EET 87720,41. Thus, the EET 87720,41 ferroan lithic clast
471 is quite distinct from brachinites.
472

473 Two pyroxene clasts from EET 83309,51 have anomalous O isotopic compositions, Gr1 and
474 Gr20 (Table 3). Grain Gr1 plots within the field of EH and EL chondrites and aubrites (Clayton
475 and Mayeda, 1996; Clayton et al., 1984). This grain is nearly pure enstatite ($Wo_{0.3}En_{99.2}Fs_{0.5}$)
476 with very low minor element contents (Al_2O_3 0.11 wt%; TiO_2, Cr_2O_3, MnO and Na_2O all <0.01
477 wt%). This composition is similar to those of orthopyroxenes in EH and EL chondrites and
478 aubrites (Brearely and Jones, 1998; Mittlefehldt et al., 1998). While Gr1 plausibly was derived
479 from an enstatite chondrite or achondrite impactor, we cannot be more specific than that. We
480 found other pyroxenes with high mg# (~98-100) and minor element contents similar to those of
481 Gr1 in DaG 999, EET 83309, EET 87720, Nilpena and North Haig; all possible debris from an
482 enstatite chondrite or achondrite parent asteroid.
483

484 Grain Gr20 has an O isotopic composition similar to those of winonaites and silicates in IAB
485 irons (Clayton and Mayeda, 1996) and has a mg# (93.5) within the range of those in these
486 meteorites (Mittlefehldt et al., 1998). However, the CaO content of Gr20 is 2.5-3.4 times those of
487 winonaite-IAB orthopyroxenes, and Al_2O_3 and Cr_2O_3 are higher and TiO_2 lower in the Gr20
488 compared to orthopyroxenes in these other meteorites (Benedix et al., 2005). Therefore, grain
489 Gr20 is not likely to be from the winonaite/IAB silicate parent asteroid. Grain Gr20 has minor
490 element contents like those of ureilitic pyroxenes and plots on the ureilite Fe/Mn-Fe/Mg trend
491 (Fig. 6), but because of its anomalous O isotopic composition (Fig. 8), it is not likely to be
492 ureilitic in origin. We conclude that Gr20 most likely represents debris from an unknown parent
493 object.

494

495 A group of unusual olivines is characterized by low MnO contents, mg#s in the range of 87-92,
496 and they plot well above the ureilite trend (Fig. 3). Although they have Cr_2O_3 and CaO contents
497 within the range of normal ureilitic olivines, we concur with Ikeda et al. (2000) and Jaques and
498 Fitzgerald (1982) that these are most likely chondritic debris. We also found one nearly pure
499 forsterite grain (mg# 99.2) with Cr_2O_3 and MnO contents at the detection limits and low CaO
500 content; it is shown on figure 3 at Fe/Mn of ~110. This grain is clearly foreign debris on the
501 ureilite parent asteroid. Possibly, it was derived from an enstatite chondrite- or achondrite-like
502 parent, although these are olivine-poor.
503
504 The exotic mineral and lithic clasts analysed for oxygen isotopes and electron microprobe are
505 derived from a variety of parent bodies and must have been present as meteoritic debris on the
506 surface of the ureilite asteroid. Thus, polymict ureilites contain minor amounts of materials that
507 originated from different parent bodies, some of which may not completely match the currently
508 sampled meteorite groups (Kita et al., 2004). We estimate that at least six impactor bodies are
509 represented; R chondrite, low-Mn ordinary chondrite (Ikeda et al., 2003), enstatite clan,
510 carbonaceous clan (dark clasts; Clayton and Mayeda, 1988; Prinz et al., 1987), the grain Gr20
511 parent and angrites (Prinz et al., 1986; Kita et al., 2004). This is different from observations of
512 the HED regolith, where only two impactors seem to dominate - CM and CR chondrites
513 (Zolensky et al., 1996) – and these likely represent a fairly narrow range of the solar system
514 judging by their similar chemistries and O isotopic compositions. The foreign debris in ureilites
515 not only was derived from a greater number of sources, but the range in O isotopic composition
516 and chemistry implies that they sample a much wider range of the solar system, including both
517 reduced and oxidized regions.
518
519 *5.2 One or more ureilite parent asteroids?*
520
521 Scott et al. (1993) and Warren and Kallemeyn (1992) observed that existing data did not require
522 a single ureilite parent asteroid. Goodrich et al. (2004) showed that collectively, the polymict
523 ureilites show a similar olivine core mg# distribution as the monomict suite. Nevertheless,

Warren et al. (2006) concluded that the database was insufficient to determine whether a single parent asteroid produced the ureilite suite.

The range of the main components within each individual polymict ureilite is very similar to that of the monomict sample suite (Fig. 5). We have tested this by performing a nonparametric Mann-Whitney two-tailed test on olivine mg#s. We randomly sampled 100 olivine gains from our data on DaG 999, DaG 1000, EET 83309, EET 87720, Nilpena and North Haig, and 100 randomly sampled monomict ureilites using our data plus literature data. (We eliminated suspected exogenous olivine grains, discussed above, from the database on polymict ureilites before sampling.) The null hypothesis - that the sample populations are not different - is accepted at the 99% confidence level. Thus, statistically, the olivine populations in polymict ureilites and the monomict ureilite suite are not significantly different. This is extremely unlikely to be the case if monomict ureilites were derived from a series of different parent asteroids. Oxygen isotope data for clasts in the polymict samples plot exactly within the range of monomict ureilites (Fig. 8). They also show the same anti-correlation between mg# and $\Delta^{17}O$ (Fig. 9) that is observed among monomict ureilites. These results are consistent with the chemistry of these clasts being complete matches to the range seen among monomict ureilites and support the premise that there is only one ureilite asteroid. Thus we conclude that there is only one single parent asteroid for all ureilites.

On the other hand, individual polymict ureilites can have somewhat different distributions of olivine compositions. We performed the same statistical test on endogenous olivine grains comparing the population from each meteorite to each of the others. The results are shown in Table 4. The population of olivines in Nilpena is distinct from that of each of the other polymict ureilites at the 99% confidence level. However, most polymict ureilites are not distinguishable from each other based on their olivine populations. Differences in CRE ages indicate each polymict sample was ejected from the parent asteroid in separate events, suggesting each could represent a slightly different mix of materials. Thus, it is not surprising that Nilpena is distinct. However, the similarity of olivine populations in most polymict ureilites suggests that the regolith is fairly well mixed, and the suite of clasts in each individual polymict ureilite is representative of the material on the parent asteroid within reach of impact gardening.

555

556 Polymict ureilites are clastic breccias. A study of their constituent minerals is therefore
557 analogous to provenance studies of terrestrial clastic sedimentary rocks such as sandstones and
558 conglomerates. In such studies, lithic clasts or grains within sedimentary rocks represent material
559 exposed within the hinterland from which the sediment was derived. Polymict ureilites have been
560 formed near the surface of the ureilite parent asteroid, and those that contain implanted solar
561 wind gases have been formed on the surface, so the range of mineral compositions represents the
562 variety of composition of the rocks present within the outer reaches of the asteroidal surface. A
563 single ureilitic lithic clast in North Haig had an area of 7 x 6 mm and one from DaG 1023 was 2
564 cm long. Therefore, some ureilitic clasts in polymict ureilites must commonly be 1-2 cm in
565 diameter. If most of the FRO ureilites are indeed part of a polymict breccia, then typical clast
566 sizes may be on the order of several cm in diameter for this meteorite. A significant observation
567 made in several previous studies and by us is that polymict ureilites contain both shocked and
568 unshocked ureilitic clasts, and also show a very wide range of compositions of ureilite minerals.
569 This indicates that the surface of the parent asteroid(s) comprises rocks of many different
570 compositions and widely varying levels of shock. Furthermore, melt clasts representing the
571 missing basalts formed by melting of the original ureilite parent asteroid(s) have also been found
572 in polymict ureilites (Cohen et al., 2004) and non-indigenous clasts (mainly of chondritic
573 compositions) are also present (e.g. Prinz et al., 1987; Ikeda et al., 2000, 2003; this study).
574

575 In terrestrial provenance studies, certain minerals found in sandstones are considered to be
576 diagnostic of derivation from certain rock-types. In an analogous manner, certain common
577 compositions of clasts, such as the ferroan olivines and “Hughes cluster” olivines and augites,
578 can be used as “indicator minerals”. DaG 999, DaG 1000, Nilpena and EET 83309 all contain
579 olivine and augite clasts that are identical to olivines and augites from Hughes 009 and
580 lithologies in FRO 93008, FRO 90054 and FRO 90228 (Figs 3 and 7). The presence of a
581 widespread common composition such as the “Hughes cluster” is unlikely to have occurred if
582 each ureilite represents a different asteroidal body.
583

584 From the study of the distribution of different mineral compositions in the polymict ureilites
585 (Fig. 3), it is clear that the exotic ferroan olivines are also quite common. They occur as lithic

clasts in the DaG pairing group, EET 83309 and EET 87720 (this work; Cohen et al., 2004; Ikeda et al., 2000, 2003), and as mineral grains in some members of the FRO pairing group (Fioretti and Goodrich, 2001; Smith, 2002). This is unlikely to have been the case if all these samples had been derived from different parent asteroids and also supports the suggestion that the polymict ureilites were all formed on the surface of a single parent asteroid. Given the evidence discussed above that ureilites are derived from a single parent asteroid, it appears that the asteroid must have been formed in (or more probably migrated into) a region of the nebula that contained bodies that were significantly more oxidized.

5.3 Ureilite groupings?

In this section, we will examine the results of our study to see if ureilites form a single compositional suite or if they fall naturally into separate groups according to their mineralogy and/or mineral compositions. Several previous studies have divided ureilites into different groups. For example, Goodrich et al. (2004; 2007) separated olivine-pigeonite ureilites from olivine-orthopyroxene ureilites, and considered the augite-bearing lithologies to be a separate type. However, this approach cannot be applied to single mineral clasts in polymict ureilites, as it depends on information about the mineral assemblage. Berkley et al. (1980) proposed a classification of ureilites into three groups using Fe/Mg values in olivine: Group 1 has low mg# (average ~ Fo79), Group 2 has intermediate values (average ~Fo84) and Group 3 has high mg# (~ Fo91). Clayton and Mayeda (1988) showed that the different Berkley mg# groups also had distinctly different oxygen isotopic compositions. This approach would be applicable to clasts in polymict breccias, but was established at a time when far fewer ureilites were known and the classification lacks an underlying rationale.

Following Berkley et al. (1980), Mittlefehldt et al. (2005) divided ureilites into three groups using observed minima in the distribution of olivine compositions in monomict ureilites at Fo83 and Fo90 in order to test for correlations with bulk chemical properties. However, the distribution of polymict olivine compositions in this study (Fig. 5) does not support such a division as the minima do not appear in the compositional distribution of polymict clasts. Mittlefehldt et al. (2005) concluded that bulk compositional trends suggest that Berkley groups 2

and 3 could represent a single group distinct from Berkley group 1. From a study of clasts in DaG 319, Ikeda et al. (2000) separated Type I ureilites (olivine-pigeonite lithologies with core olivine mg#s < 84, reduction rims on olivines, and the presence of carbon phases) from Type II (olivine-orthopyroxene-augite assemblages, with mg#s > 85, lacking carbon and with little or no reduction around olivines). We have also observed that ureilite olivines with mg#s < 85 are far more common than those with mg#s > 85 (Fig. 5), so a separation into two groups appears to be well founded. In fact, the bimodal distribution observed in olivine composition data for monomict ureilites and clasts in polymict ureilites may indicate that there are two overlapping distribution curves, one centered on Fo78 and the other centered on Fo87.

The difference between the two groups of ureilitic olivines can be seen more clearly in the relation between their Fe and Mn contents in Fig. 10. As discussed by Karner et al. (2003), olivines that have crystallized from basaltic melts show positive correlations in this figure. However, most olivine clasts from polymict ureilites form a relatively tight negative correlation between Fe and Mn, similar to that displayed by olivines from the majority of monomict ureilites. All of these olivines have mg#s < 85 and most have Mn contents < 0.0105 afu (only three olivine clasts have higher Mn contents). In contrast, data for olivines with mg# > 85 are much more scattered, both for monomict samples and clasts in polymict ones. This scattered group includes the highly magnesian olivine-augite-pigeonite clast in DaG 999, the unusual paired monomict augite-bearing ureilites ALH 83120 and ALH 81206 (which are also paired with ALH 84136) and the low-Mn ureilites Y-74659 and EET 87517 (the latter also augite-bearing). High-Mn contents of olivines also appear in the “Hughes cluster”, i.e. monomict augite-bearing ureilites Hughes 009, EET 96314, EET 96331, EET 96293, and FRO 90054, FRO 90228 and one lithology in FRO 93008 of the possibly polymict FRO pairing group, together with olivine clasts from polymict ureilites that have very similar compositions.

Figure 10 also shows that the compositional range of olivine clasts in polymict ureilites is very similar to that of monomict ureilites, even including low-Fe, low-Mn olivines similar to those of EET 87517 and Y-74659. Only a few clasts plot outside the range of monomict olivine compositions, mainly to higher Mn contents. Whether monomict ureilites of a composition similar to the large augite-bearing ureilitic clast in DaG 999 will be found in the future remains

an open question. However, Figs. 5 and 10 suggest that most new ureilite finds will plot in the main group with olivine mg#s < 85.

As is the case for terrestrial ultramafic rocks, ureilites could simply be classified on the basis of their modal proportions. The boundary between peridotite and pyroxenite is at 40% olivine (Streckeisen, 1976). Although modal proportions of phases in ureilites are hard to estimate because of the coarse grain-size and the small areas of typical petrographic thin-sections, nevertheless it is clear that the vast majority of ureilites contain > 40% olivine (see Mittlefehldt et al., 1998) and are therefore peridotites. They are in many ways analogous to harzburgites in the Earth's mantle. Only a few ureilites contain > 60% pyroxene (e.g. LEW 88774, Hammadah al Hamra (HaH) 064, Y-74130, Hughes 009, MET 01085 and FRO 90054) and hence are technically pyroxenites. In the Earth's mantle, the distinction between pyroxenite and peridotite is fundamental; peridotites are broadly speaking restites after partial melting, whereas pyroxenites generally form by magmatic processes (e.g. crystal accumulation, melt impregnation).

A further distinction that can be made among monomict ureilites is a textural one. Most ureilites display a granoblastic texture with triple junctions between silicate crystals and metal along grain boundaries (Berkley, 1986). However, a few ureilites (e.g. Pecora Escarpment (PCA) 82506, Reckling Peak (RKPA) 80239 and LEW 85440) have poikilitic textures. Poikilitic low-Ca pyroxene is also closely associated with the "bimodal" texture reported in META 78008, Y-74130, EET 87511 and ALH 82130 (Mittlefehldt et al., 1998). Other poikilitic or bimodal ureilites that have not been well studied yet include DaG 879 and FRO 01088. The paired Antarctic ureilites EET 87511, EET 87523, EET 87717, EET 96322, EET 96328 and EET 96262 all show poikilitic textures. Augite poikilitically encloses olivine in the augite-bearing low-carbon lithology of FRO 93008. Clasts of poikilitic ureilite in Northwest Africa (NWA) 1926 (a fragmental ureilitic breccia) also contain very little carbon. Ureilites that show this texture probably formed by a different petrogenetic process than those that show more typical ureilitic textures. The texture generally is strongly reminiscent of that of some terrestrial igneous cumulates and Goodrich (1986) has interpreted poikilitic textures in orthopyroxene- and augite-

678 bearing ureilites as being due to cumulus processes. We will now consider the significance of
679 augite in ureilites and the nature of the "Hughes cluster".
680
681 *5.4 Augite-bearing ureilites and the "Hughes cluster"*
682
683 Takeda et al. (1989) first drew attention to the unusual nature of augite-bearing ureilites.
684 According to Mittlefehldt et al. (1998) and Goodrich et al. (2004), there are eight augite-bearing
685 monomict ureilites: Hughes 009, LEW 85440 (paired with LEW 88012, LEW 88201, LEW
686 88281), ALH 82106 (paired with ALH 82130, ALH 84136), EET 87511 (paired with EET
687 87523, EET 87717), HaH 064, META78008, Y-74130 and LEW 88774. Furthermore, we have
688 found that Antarctic ureilites EET 87517, EET 96293, EET 96314 and EET 96331 contain
689 augite. Augite-bearing lithologies from the probable polymict ureilites FRO 90054, FRO 90228
690 and FRO 93008 can be added to this list (Smith, 2002). One large clast in DaG 999 also
691 represents a highly magnesian (mg# = 97) augite-bearing ureilitic lithology. Figure 7
692 demonstrates that augites from monomict ureilites show a wide range of mg#s, from the highly
693 magnesian ones in ALH 82106/ALH 82130 (mg# = 95), which closely resemble the augite-
694 bearing clast in DaG 999, through the "Hughes cluster" compositions, to a group of monomict
695 ureilites with more iron-rich augites (HaH 064, META78008, LEW 88774, Y-74130) with mg#s
696 of 76. As discussed above, three of these samples are pyroxenites rather than peridotites. Their
697 augites have distinctly lower Ca contents than those of the more Mg-rich varieties (Fig.7) and,
698 curiously, do not appear to have given rise to clasts in polymict breccias. Goodrich (1986)
699 suggested that the augite in Y-74130 was cumulus in origin. Augite has also been found in
700 interstitial material, interpreted as melt veins, in monomict ureilites Y-74123 and Y-790981
701 (Ogata et al., 1991).
702
703 The augite-bearing Hughes 009 contains melt inclusions hosted by olivine crystals and lacks
704 carbon phases (Goodrich et al., 2001). FRO 90054, FRO 90228 and the olivine-augite-
705 orthopyroxene lithology in FRO 93008 also all contain little carbonaceous material (Smith,
706 2002) and melt inclusions have been reported from FRO 90054 (Fioretti and Goodrich, 2000;
707 Goodrich, 2001). The high Mn/Mg ratios of olivines in all these augite-bearing ureilites resemble
708 those of olivine in igneous-textured augite-olivine clasts in polymict ureilites reported by Cohen

et al. (2004). This interpretation is supported by the existence of ureilitic pyroxene clasts in polymict ureilites that form an igneous fractionation trend away from the "Hughes cluster", identical to the trend observed by Cohen et al. (2004) in pyroxenes from melt clasts (Fig. 6). This trend of increasing Fe/Mg with nearly constant Fe/Mn is an igneous fractionation trend exhibiting no evidence for FeO reduction (see Mittlefehldt, 1986). Thus, it is most likely that the augite-bearing "Hughes cluster" was formed by melt-related processes on the ureilite parent asteroid as advocated by Goodrich et al. (2001) for Hughes 009. The presence of augite crystals at triple junctions in the paired monomict ureilites EET 96293, EET 96314 and EET 96331 suggests that melt impregnation processes occurred in these samples, i.e. they were derived by interaction of an augite-bearing melt and restitic mantle minerals. The textures are identical to that in Hughes 009 itself (Goodrich et al., 2001). However, it is unlikely that all ureilites with mg#s > 85 were formed by melt impregnation, as not all contain augite, and such an explanation cannot account for the low Mn contents of olivines in Y-74659 and EET 87517.

6. Conclusions

A petrological study of ureilitic silicate mineral clasts in six polymict ureilites has revealed that each polymict ureilite contains a wide range of olivine and pyroxene compositions, exactly covering the Fe-Mg-Mn compositional range seen among monomict ureilites. The olivine mg# distribution in the studied polymict ureilites is statistically indistinguishable from that of the monomict ureilite suite, indicating they sample the same olivine population. SIMS oxygen isotope data for clasts from two polymict samples also cover the range shown by bulk analyses of monomict ureilites. "Indicator minerals", such as olivines and augites derived from material similar to the monomict ureilite Hughes 009, are present in several different polymict ureilites. Together, these observations are interpreted to indicate that all ureilites were derived from a single parent asteroid.

Exotic ferroan olivines derived from R-chondrites and another oxidized asteroid are also present on the surface of the ureilite asteroid, as also confirmed by the SIMS oxygen isotope analyses. Mineral compositions and O isotope data show that enstatite chondrite or achondrite materials, and material from an unknown meteorite type are present, and petrologic evidence shows that

740 other exogenous grains are present. Combining our and literature data, we estimate that at least
741 six distinct impactor types are represented in the polymict breccias.
742
743 Ureilites fall into two main groups, according to the mg# and Mn contents of their olivines.
744 Those with mg# <85 show a coherent negative trend of FeO vs. MnO in olivines, whereas those
745 with mg#s >85 are much more scattered. The more magnesian group includes the "Hughes
746 cluster" materials, which contain melt inclusions. These data are interpreted to indicate that
747 magnesium-rich partial melts were still present in the ureilite asteroid when it was disrupted by
748 impact, and these melts became impregnated into the residual mantle to form "Hughes cluster"
749 rocks.
750
751 After disruption, a daughter ureilite asteroid accreted at a much lower temperature, forming a
752 rubble-pile body. The occurrence of mafic silicate minerals showing a wide range of mg#s in all
753 of the polymict ureilites investigated in this study indicates that all of this material was within
754 impact gardening depth of the surface of the daughter asteroid during regolith formation.
755 Material of various shock levels was also exposed on the surface of the asteroid. Regolith
756 formation began and impacts from a wide range of other bodies occurred, including showers of
757 material from both more oxidized and more reduced asteroids.
758
759 **Acknowledgements**
760
761 We thank the Meteorite Working Group for providing the EET samples, Alex Bevan for the
762 sections of North Haig, Luigi Folco for the Frontier Mountains samples and Cyrena Goodrich for
763 loaning the sections of Nilpena and providing data for Figure 5. Barbara Cohen kindly provided
764 the data for minerals in melt clasts. DaG samples were purchased from Erich Haiderer. We thank
765 Craig Schwandt and GeorgAnn Robinson for help with the SEM and electron microprobe,
766 respectively. Discussions with colleagues at LPI and JSC were very stimulating and helpful.
767 This work was supported by the Lunar and Planetary Institute (HD) and the NASA
768 Cosmochemistry Program (DWM). The WiscSIMS ion microprobe lab is supported by NSF
769 (EAR-0319230, 0509639).
770

Figure captions

Fig.1 BSE images of sections of two polymict ureilites (EET 83309, EET 87720) examined in this study. Clasts analysed by SIMS for oxygen isotopes are indicated. Also indicated is an exotic "granitic" clast composed of an intimate intergrowth of albite and a silica polymorph.

Fig.2. Fe/Mn vs. Fe/Mg molar compositions of olivines from monomict ureilites analysed at JSC using the same analytical protocol used in this study (Hudon and Mittlefehldt, data in EA-2), a single ureilite clast in DaG 1023 (demonstrating reproducibility of the analytical technique), and two different lithologies in FRO 93008, compared with the ureilite trend of Goodrich et al. (2004) (solid line).

Fig.3. Fe/Mn vs. Fe/Mg molar compositions of all olivines from clasts and single mineral grains analysed from polymict ureilites in this study compared to the ureilite trend of Goodrich et al. (2004) (solid line).

Fig.4. Fe/Mn vs. Fe/Mg molar compositions of ureilitic olivines from six individual polymict ureilite meteorites analysed in this study.

Fig.5. Histogram of Fo content of olivine in ureilitic clasts and single mineral grains from polymict ureilites in this study, compared with the distribution of olivine compositions in monomict ureilites given by Goodrich et al. (2004).

Fig.6. Fe/Mn vs. Fe/Mg molar compositions of pyroxenes from monomict and polymict ureilites analysed in this study and by Hudon and Mittlefehldt (data in EA-2). The field of melt clast pyroxene compositions is based on analyses by Cohen et al. (2004).

Fig.7. Ca (afu) vs. mg# for pyroxenes from monomict and polymict ureilites analysed in this study and by Hudon and Mittlefehldt (data in EA-2). The field of melt clast pyroxene compositions is based on analyses by Cohen et al. (2004).

802 Figure 8. Oxygen three isotope compositions of clasts in polymict ureilites EET 83309 and
803 EET87720. Ureilitic clasts are shown as open symbols (olivine-square, pyroxene-circle) and
804 EET87720, 41 Gr38, which belongs to the "Hughes cluster" is marked as a crossed square. Non-
805 ureilitic clasts are shown as filled symbols (ferroan clasts –square and enstatite-circle). Three
806 lines labeled as "TF", "CCAM" and "Y&R" are Terrestrial mass fractionation line ($\delta^{17}O=0.52 \times$
807 $\delta^{18}O$), carbonaceous chondrite anhydrous mineral line (Clayton and Mayeda, 1999) and Young
808 and Russell line (Young and Russell, 1998). Small dots and shadowed areas are from monomict
809 ureilite bulk analyses (Clayton and Mayeda, 1996) and crosses are bulk R-chondrites (Weisberg
810 et al., 1991; Bischoff et al., 1994; Schultz et al., 1994). Error bars are 2 sigma.
811
812 Figure 9. Relationship between mg# and $\Delta^{17}O$ among ureilitic clasts. Symbols for polymict
813 ureilite data are the same as in Fig. 8. The monomict ureilite data (Clayton and Mayeda, 1996)
814 are shown as small filled diamonds. Note that EET83309, 51 Gr20 deviates significantly from
815 the ureilite trend as in Fig. 8.
816
817 Figure 10. FeO vs. MnO (wt%) contents in ureilitic olivines from monomict and polymict
818 ureilites analyzed here and by Hudon and Mittlefehldt (data in EA-2) with literature data from
819 Goodrich et al (1987), Treiman and Berkley (1994), Takeda (1986), Torigoye-Kita et al (1995),
820 Smith (2002) and Singletary and Grove (2003). Magnesian monomict ureilites that contain
821 augite are shown in bold and underlined.
822
823 REFERENCES
824
825 Benedix, G.K., Lauretta, D.S., McCoy, T.J., 2005. Thermodynamic constraints on the formation
826 conditions of winonaites and silicate-bearing IAB irons. *Geochim. Cosmochim. Acta* **69**, 5123-
827 5131.
828
829 Berkley, J.L., 1986. Four Antarctic ureilites: petrology and observations on ureilite petrogenesis.
830 *Meteoritics* **21**, 169-189.
831

832 Berkley, J.L., Taylor, G.J., Keil, K., Harlow, G.E., Prinz, M., 1980. The nature and origin of
833 ureilites. *Geochim. Cosmochim. Acta* **44**, 1579-1597.
834
835 Bischoff, A., Geiger, T., Palme, H., Spettel, B., Schultz, L., Scherer, P., Loeken, T., Bland, P.,
836 Clayton, R.N., Mayeda, T.K., Herpers, U., Meltzow, B., Michel, R., Dittrich-Hannen, B., 1994.
837 Acfer 217 – A new member of the Rumuruti chondrite group (R) *Meteoritics* **29**, 264-274.
838
839 Brearley, A.J., Jones, R.H., 1998. Chondritic meteorites. In: *Planetary Materials.* (ed. J.J.
840 Papike), *Rev. Mineral.* **36**, 3-1 – 3-398. Mineralogical Society of America, Washington, D.C.
841
842 Brearley, A.J., Prinz, M., 1992. CI chondrite-like clasts in the Nilpena polymict ureilite:
843 implications for aqueous alteration processes in CI chondrites. *Geochim. Cosmochim. Acta* **56**,
844 1373-1386.
845
846 Clayton, R.N., Mayeda, T.K., 1988. Formation of ureilites by nebular processes. *Geochim.*
847 *Cosmochim. Acta* **52**, 1313-1318.
848
849 Clayton, R.N., Mayeda, T.K., 1996.Oxygen isotope studies of achondrites. *Geochim.*
850 *Cosmochim. Acta* **60**, 1999-2017.
851
852 Clayton, R.N., Mayeda, T.K., Rubin, A.E., 1984. Oxygen isotopic compositions of enstatite
853 chondrites and aubrites. *Proc. 15th Lunar Planet. Sci. Conf., Part 1, J. Geophys. Res.* **89** (Suppl.),
854 C245-C249.
855
856 Cohen, B., Goodrich, C.A., Keil, K., 2004. Feldspathic clast populations in polymict ureilites:
857 Stalking the missing basalts from the ureilite parent body. *Geochim. Cosmochim. Acta* **68**, 4249-
858 4266.
859
860 Fioretti, A.M., Goodrich, C.A., 2000. Primary melt inclusions in olivine, augite and
861 orthopyroxene in ureilite FRO 90054. *Lunar Planet. Sci.* **31**, #1202.
862

Fioretti, A.M., Goodrich, C.A., 2001. A contact between an olivine-pigeonite lithology and an olivine-augite-orthopyroxene lithology in ureilite FRO 93008: dashed hopes? *Meteoritics Planet. Sci.* **36,** A58.

Fioretti, A.M., Molin, G., 1996. Petrography and mineralogy of FRO 93008 ureilite: evidence for pairing with FRO 90054 ureilite. *Meteoritics Planet. Sci.* **31,** A43.

Goodrich, C.A., 1986. Y74130: a ureilite with cumulus augite. *Meteoritics* **21**, 373-374.

Goodrich, C.A., 1992. Ureilites – a critical review. *Meteoritics* **27**, 327-352.

Goodrich, C.A., 1999. A primary silicate mineral/melt reaction texture in ureilite Lewis Cliff 88774. *Meteoritics Planet. Sci.* **34,** A44-A45.

Goodrich, C.A., 2001. Magmatic inclusions in Frontier Mountains 90054 and Elephant Moraine 96328: complex petrogenesis of the olivine-(augite)-orthopyroxene ureilites. *Lunar Planet. Sci.* **32**, #1300.

Goodrich, C.A., Jones, J.H., Berkley, J.L., 1987. Origin and evolution of ureilite parent magmas: Multi-stage igneous activity on a large parent body. *Geochim. Cosmochim. Acta* **51**, 2255-2273.

Goodrich, C.A., Fioretti, A.M., Tribaudino, M., Molin, G., 2001. Primary trapped melt inclusions in olivine in the olivine-augite-orthopyroxene ureilite Hughes 009. *Geochim. Cosmochim. Acta* **65**, 621-652.

Goodrich, C.A., Hutcheon, I.D., Keil, K., 2002. ^{53}Mn-^{53}Cr age of a highly evolved, igneous lithology in polymict ureilite DaG 165. *Meteoritics Planet. Sci.* **37**, A54.

Goodrich, C.A., Scott, E.R.D., Fioretti, A.M., 2004. Ureilitic breccias: clues to the petrological structure and impact disruption of the ureilite parent asteroid. *Chemie der Erde* **64**, 283-327.

894 Goodrich, C.A., Van Orman, J. A, Wilson, L., 2007. Fractional melting and smelting on the
895 ureilite parent body. *Geochim. Cosmochim. Acta***71**, 2876-2895.
896
897 Guan, Y., Crozaz, G., 2000. Light rare earth element enrichments in ureilites: a detailed ion
898 microprobe study. *Meteoritics Planet. Sci.* **35**, 131-144.
899
900 Guan, Y., Crozaz, G., 2001. Microdistributions and petrogenetic implications of rare earth
901 elements in polymict ureilites. *Meteoritics Planet. Sci.* **36**, 1039-1956.
902
903 Ikeda, Y., Prinz, M., 2001. Magmatic inclusions and felsic clasts in the Dar al Gani 319 polymict
904 ureilite. *Meteoritics Planet. Sci.* **36**, 481-499.
905
906 Ikeda, Y., Prinz, M., Nehru, C.E., 2000. Lithic and mineral clasts in the Dar al Gani (DAG) 319
907 polymict ureilite. *Antarctic Meteorite Res.* **13**, 177-221.
908
909 Ikeda, Y., Kita, N.T., Morishita, Y., Weisberg, M.K., 2003. Primitive clasts in the Dar al Gani
910 319 polymict ureilite: Precursors of the ureilites. *Antarctic Meteorite Res.* **16**, 105-127.
911
912 Jaques, A.L., Fitzgerald, M.J., 1982. The Nilpena ureilite, an unusual polymict breccia:
913 implications for origin. *Geochim. Cosmochim. Acta* **46**, 893-900.
914
915 Karner, J., Papike, J.J., Shearer, C.K., 2003. Olivine from planetary basalts: chemical signatures
916 that indicate planetary parentage and those that record igneous setting and process. *Am. Min.* **88**,
917 806-816.
918
919 Kita, N.T., Ikeda, Y., Morishita, Y., Togashi, S., 2003. Timing of basaltic volcanism in ureilite
920 parent body inferred from the ^{26}Al ages of plagioclase-bearing clasts in DaG0319 polymict
921 ureilite. Lunar Planet Sci. **34,** #1557.
922

Kita, N.T., Ikeda, Y., Togashi, S., Liu, Y., Morishita, Y., Weisberg, M.K., 2004. Origin of ureilites inferred from a SIMS oxygen isotopic and trace element study of clasts in the Dar al Gani 319 polymict ureilite. *Geochim. Cosmochim. Acta* **68**, 4213-4235.

Kita, N. T., Ushikubo, T., Fu, B., Spicuzza, M.J., Valley J.W., 2007. Analytical developments on oxygen three isotope analyses using a new generation ion microprobe ims-1280. *Lunar Planet. Sci.* **38**, #1981.

Lee, D.-C., Halliday, A.N., Singletary, S.J., Grove, T.L., 2005. ^{182}Hf-^{182}W chronometry and an early differentiation in the parent body of ureilites. *Lunar Planet. Sci.* **36**, #1638.

Mason, B., 1986. Sample No. EET83309. *Antarctic Meteorite Newslet.* **9,** No. 1, 15.

Mittlefehldt, D.W., 1986. Fe-Mg-Mn relations of ureilite olivines and pyroxene and the genesis of ureilites. *Geochim. Cosmochim. Acta* **50**, 107-110.

Mittlefehldt, D.W., Lindstrom, M.M., 2001. Petrology and geochemistry of Patuxent Range 91501, an impact melt from the L chondrite parent body, and Lewis Cliff 88663, an L7 chondrite. *Meteoritics Planet. Sci.* **36**, 439-457.

Mittlefehldt, D.W., McCoy, T.J., Goodrich, C.A., Kracher, A., 1998. Non-chondritic meteorites from asteroidal bodies. In: *Planetary Materials.* (ed. J.J. Papike), *Rev. Mineral.* **36**, 4-1 – 4-195. Mineralogical Society of America, Washington, D.C.

Mittlefehldt, D.W., Bogard, D.D., Berkley, J.L., Garrison, D.H., 2003. Brachinites: Igneous rocks from a differentiated asteroid. *Meteoritics Planet. Sci.* **38**, 1601-1625.

Mittlefehldt, D.W., Hudon, P., Galindo, C., Jr., 2005. Petrology, geochemistry and genesis of ureilites. *Lunar Planet. Sci.* **36**, #1040.

953 Ogata, H., Mori, H., Takeda, H., 1991. Mineralogy of interstitial rim materials of the Y74123
954 and Y790981 ureilites and their origin. *Meteoritics* **26**, 195-201.
955
956 Prinz, M., Weisberg, M.K., Nehru, C.E., Delaney, J.S., 1986. North Haig and Nilpena: paired
957 polymict ureilites with Angra dos Reis-related and other clasts. *Lunar Planet. Sci.* **17**, 681-682.
958
959 Prinz, M., Weisberg, M.K., Nehru, C.E., Delaney, J.S., 1987. EET83309, a polymict ureilite:
960 recognition of a new group. *Lunar Planet. Sci.* **18**, 802-803.
961
962 Rai, V.K., Murthy, A.V.S., Ott, U., 2003. Noble gases in ureilites: cosmogenic, radiogenic and
963 trapped components. *Geochim. Cosmochim. Acta* **67**, 4435-4456.
964
965 Russell, S.S., Zipfel, J., Folco, L., Jones, R., Grady, M.M., McCoy, T., Grossman, J.N., 2003.
966 The Meteoritical Bulletin, No 87, *Meteoritics Planet. Sci.* **38**, A189-A248.
967
968 Schulze, H., Bischoff, A., Palme, H., Spettel, B., Dreibus, G., Otto, J., 1994. Mineralogy and
969 chemistry of Rumuruti: The first meteorite fall of the new R chondrite group. *Meteoritics* **29**,
970 275-286.
971
972 Schwarz, C., Mason, B., 1989. Sample No. EET87720. *Antarctic Meteorite Newslet.* **12,** No. 3,
973 15.
974
975 Scott, E.R.D., Taylor, G.J., Keil, K., 1993. Origin of ureilite meteorites and implications for
976 planetary accretion. *Geophys. Res. Lett.* **20**, 415-418.
977
978 Singletary, S.J., Grove, T.L., 2003. Early petrologic processes on the ureilite parent body.
979 *Meteoritics Planet. Sci.* **38**, 95-108.
980
981 Smith, C.L., Wright, I.P., Franchi, I.A., Grady, M.M., 2000. A statistical analysis of
982 mineralogical data from Frontier Mountains ureilites. *Meteoritics Planet. Sci.* **35**, A150.
983

984 Smith, C.L., 2002. An integrated, mineralogical, petrologic and isotopic study of ureilites. PhD
985 dissertation, Open University.
986
987 Streckeisen, A., 1976. To each plutonic rock its proper name. *Earth Sci. Rev.* **12**, 1-33.
988
989 Takeda, H., 1986. Mineralogy of Antarctic ureilites and a working hypothesis for their origin and
990 evolution. *Earth Planet Sci Lett* **81**, 358-370.
991
992 Takeda, H., Mori, H., Ogata, H., 1989. Mineralogy of augite-bearing ureilites and the origin of
993 their chemical trends. *Meteoritics* **24**, 73-81.
994
995 Torigoye-Kita, N., Tatsumoto, M., Meeker, G.P., Yanai, K., 1995. The 4.56 Ga U-Pb age of the
996 MET 78008 ureilite. *Geochim. Cosmochim. Acta* **59**, 2319-2329.
997
998 Treiman, A.H., Berkley, J.L., 1994. Igneous petrology of the new ureilites Nova 001 and
999 Nullabor 010. *Meteoritics* **29**, 843-848.
1000
1001 Walker D, Grove T L, 1993. Ureilite smelting. *Meteoritics* **28,** 629-636.
1002
1003 Warren, P.H., Huber, H., 2006. Ureilite petrogenesis: A limited role for smelting during anatexis
1004 and catastrophic disruption. *Meteoritics Planet. Sci.* **41**, 835-849.
1005
1006 Warren , P. H., Ulff-Moller F, Huber, H., Kallemey,n G. W., 2006. Siderophile geochemistry of
1007 ureilites: A record of early stages of planetesimal core formation. *Geochim. Cosmochim. Acta*
1008 **70,** 2104-2126.
1009
1010 Warren, P., Kallemeyn, G.W., 1989. Geochemistry of polymict ureilite EET83309, and a
1011 partially-disruptive impact model for ureilite origin. *Meteoritics* **24**, 233-246.
1012
1013 Warren, P., Kallemeyn, G.W., 1992. Explosive volcanism and the graphite-oxygen fugacity
1014 buffer on the parent asteroid(s) of the ureilite meteorites. *Icarus* **100**, 110-126.

Weber, I., Bischoff, A., 1998. Mineralogy and chemistry of the ureilites Hammadah al Hamra 064 and Jalanash. *Lunar Planet. Sci.* **29**, #1365.

Weisberg, M.K., Prinz, M., Kojima, H., Yanai, K., Clayton, R.N., Mayeda, T.K., 1991. The Carlisle Lakes-type chondrites: A new grouplet with high $\Delta^{17}O$ and evidence for nebular oxidation. *Geochim. Cosmochim. Acta* 55, 2657-2669.

Welten, K.C., Nishiizumi, K., Caffee, M.W., Hillegonds, D.J., 2006. Cosmogenic radionuclides in ureilites from Frontier Mountains, Antarctica: evidence for a polymict breccia. *Lunar Planet. Sci.* **37**, #2391.

Young, E.D., Russell, S.S., 1998. Oxygen reservoirs in the early solar nebula inferred from an Allende CAI. *Science* **282,** 452-455.

Zolensky, M.E., Weisberg, M.K., Buchanan, P.C., Mittlefehldt, D.W., 1996. Mineralogy of carbonaceous chondrite clasts in HED achondrites and the moon. *Meteoritics Planet. Sci.* **31**, 518-537.

Zolensky M E, Weisberg M K, Buchanen P C and Mittlefehldt D W 1996. Mineralogy of carbonaceous chondrite clasts in HED achondrites and the Moon. *Meteoritics* **31**, 518-537.

Table 1. Representative electron microprobe analyses of olivine grains in polymict ureilites. * = Hughes cluster; ** = DaG 999 ol-aug-pig clast

Sample	grain	SiO_2	Cr_2O_3	FeO	MnO	MgO	CaO	sum	Fe/Mn	Fe/Mg	mg#
Ureilitic olivines											
DaG 999	gr 45	37.81	0.58	19.91	0.42	40.51	0.32	99.54	47.35	0.28	78.39
DaG 999	gr 103	38.11	0.87	19.00	0.60	40.32	0.49	99.40	31.12	0.26	79.09
DaG 999	gr 35	38.74	0.75	18.69	0.43	40.22	0.37	99.20	42.74	0.26	79.32
DaG 999	gr 9	38.91	0.79	17.50	0.44	41.20	0.39	99.23	39.11	0.24	80.76
DaG 999	gr 88	39.41	0.74	16.28	0.45	42.24	0.38	99.49	35.98	0.22	82.22
DaG 999	gr 40*	40.04	0.59	12.76	0.59	45.20	0.29	99.48	21.29	0.16	86.32
DaG 999	gr 34	40.16	0.72	11.07	0.46	46.60	0.36	99.37	23.70	0.13	88.24
DaG 999	gr 77	40.46	0.74	9.62	0.47	47.73	0.36	99.39	20.19	0.11	89.84
DaG 999	gr 43	41.27	0.21	6.20	0.64	50.64	0.19	99.15	9.57	0.07	93.57
DaG 999	gr 26**	41.96	0.42	2.71	0.46	53.11	0.29	98.95	5.85	0.03	97.21
DaG 1000	gr23 A	38.12	0.71	22.63	0.41	37.71	0.39	99.97	54.04	0.34	74.81
DaG 1000	gr20	38.30	0.81	22.00	0.42	38.12	0.42	100.06	52.01	0.32	75.54
DaG 1000	gr16	38.58	0.60	20.80	0.45	39.26	0.29	99.97	45.98	0.30	77.08
DaG 1000	gr15	38.55	0.58	19.95	0.42	39.95	0.31	99.77	46.64	0.28	78.11
DaG 1000	gr19	41.15	0.65	8.32	0.47	49.18	0.35	100.12	17.35	0.09	91.33
DaG 1023	gr1	38.75	0.73	18.16	0.41	40.92	0.33	99.30	43.41	0.25	80.07
EET83309	,51 gr29	37.80	0.76	23.80	0.41	37.11	0.40	100.28	56.72	0.36	73.53
EET83309	,51 gr9	38.46	0.70	21.57	0.42	39.05	0.35	100.55	50.71	0.31	76.34
EET83309	,50 gr22	38.23	0.74	20.79	0.42	39.48	0.38	100.03	48.95	0.30	77.20
EET83309	,50 gr84	38.03	0.74	20.48	0.42	39.68	0.38	99.73	48.49	0.29	77.55
EET83309	,51 gr19	38.98	0.79	19.13	0.43	40.98	0.37	100.69	43.80	0.26	79.25
EET83309	,50 gr60	38.55	0.75	15.83	0.41	43.33	0.33	99.20	37.97	0.21	82.99
EET83309	,51 gr26	40.08	0.77	13.13	0.47	45.88	0.37	100.70	27.69	0.16	86.16
EET87720	,41 gr15	38.17	0.68	22.78	0.41	37.67	0.35	100.07	54.36	0.34	74.67
EET87720	,41 gr37	38.18	0.77	22.41	0.42	37.74	0.44	99.95	52.96	0.33	75.02
EET87720	,41 gr44	38.24	0.87	22.04	0.42	37.95	0.44	99.96	51.28	0.33	75.42
EET87720	,41 gr28	38.51	0.68	21.32	0.42	38.79	0.36	100.08	49.66	0.31	76.43
EET87720	,41 gr48	38.50	0.76	20.83	0.44	39.08	0.40	100.01	47.24	0.30	76.98
EET87720	,41 gr30	38.78	0.76	20.41	0.43	39.49	0.37	100.25	46.87	0.29	77.52
EET87720	,41 gr33	38.90	0.71	19.49	0.44	40.36	0.35	100.25	43.51	0.27	78.68
EET87720	,41 gr20	39.02	0.81	19.19	0.44	40.50	0.39	100.34	43.19	0.27	79.00
EET87720	,41 gr50	38.98	0.84	18.99	0.44	40.57	0.37	100.19	42.89	0.26	79.20
EET87720	,41 gr69	39.18	0.77	18.78	0.44	40.92	0.38	100.47	42.28	0.26	79.52
EET87720	,41 gr40	39.02	0.76	18.41	0.43	41.17	0.37	100.16	42.60	0.25	79.94
EET87720	,41 gr76	39.29	0.88	17.78	0.45	41.73	0.42	100.54	39.35	0.24	80.71
EET87720	,41 gr41	39.28	0.81	17.60	0.45	41.62	0.38	100.15	38.61	0.24	80.82
EET87720	,41 gr60	39.45	0.77	16.93	0.44	42.26	0.35	100.19	37.58	0.22	81.65
EET87720	,41 gr21	39.36	0.81	16.36	0.46	42.65	0.39	100.02	35.50	0.22	82.29
EET87720	,41 gr65*	40.25	0.56	12.39	0.57	46.35	0.28	100.40	21.55	0.15	86.96
EET87720	,41 gr38*	40.29	0.59	11.71	0.57	46.31	0.29	99.75	20.41	0.14	87.57
EET87720	,41 gr29	40.50	0.62	10.87	0.44	47.06	0.34	99.83	24.27	0.13	88.53
FRO 93008	gr24	37.64	0.55	18.93	0.44	39.04	0.32	96.92	42.43	0.27	78.62
FRO 93008	gr2*	39.09	0.55	12.09	0.55	44.46	0.29	97.03	21.92	0.15	86.76
Nilpena	A gr 24	37.44	0.54	24.28	0.42	36.73	0.34	99.74	57.11	0.37	72.94
Nilpena	A gr 36	37.91	0.49	23.21	0.41	37.46	0.28	99.76	55.66	0.35	74.20
Nilpena	A gr 27	38.94	0.72	17.53	0.42	41.80	0.35	99.75	41.14	0.24	80.95
Nilpena	A gr 45	39.15	0.84	16.56	0.45	42.29	0.41	99.71	36.22	0.22	81.99
Nilpena	A gr 7	40.43	0.83	14.58	0.48	43.26	0.53	100.11	30.10	0.19	84.10
Nilpena	A gr 28	40.67	0.64	8.14	0.46	49.32	0.35	99.58	17.37	0.09	91.53
North Haig	B gr34	36.66	0.35	28.46	0.54	32.14	0.31	98.46	52.13	0.50	66.80
North Haig	B gr37	37.74	0.75	22.24	0.41	37.28	0.43	98.84	53.72	0.33	74.93
North Haig	B gr18	38.17	1.07	21.01	0.42	37.58	0.50	98.75	49.02	0.31	76.13
North Haig	B gr49	38.07	0.86	20.31	0.42	38.75	0.43	98.84	47.94	0.29	77.27
North Haig	B gr61	38.36	0.72	19.61	0.45	39.49	0.40	99.02	43.51	0.28	78.21
North Haig	B gr11	38.57	0.75	19.31	0.42	39.53	0.33	98.90	45.65	0.27	78.49
North Haig	B gr4	38.95	0.78	17.04	0.42	41.29	0.40	98.89	39.98	0.23	81.20
North Haig	B gr48	39.28	0.67	14.55	0.47	43.54	0.35	98.85	30.48	0.19	84.21
North Haig	B gr19	40.12	0.74	9.87	0.50	47.26	0.31	98.79	19.56	0.12	89.51
North Haig	B gr35	40.95	0.70	5.54	0.50	50.45	0.36	98.51	10.88	0.06	94.19
Olivines in ferroan clasts											
DaG 999	gr 109	35.72	0.03	33.17	0.41	29.77	0.09	99.19	79.58	0.63	61.53
DaG 1000	gr8	36.32	0.01	33.42	0.42	29.68	0.10	99.94	78.24	0.63	61.29
EET 83309	,51 RC	37.50	0.02	32.51	0.41	29.85	0.08	100.37	78.09	0.33	62.07
EET87720	,41 RC	36.64	0.08	31.76	0.41	31.12	0.28	100.29	76.99	1.31	63.59
Chondritic olivines											
North Haig	B gr39	42.13	0.00	0.79	0.01	55.47	0.11	98.51	107.86	0.01	99.21

Table 2 Representative electron microprobe analyses of pyroxene clasts in polymict ureilites. a = augite; ** = ol-aug=pig clast in DaG 999

Sample	grain	SiO2	TiO2	Al2O3	Cr2O3	FeO	MnO	MgO	CaO	Na2O	sum	Fe/Mn molar	Fe/Mg molar	mg#
ureilitic pyroxenes														
DaG 999	gr8	54.33	0.05	0.66	1.14	12.77	0.41	26.03	3.89	0.07	99.34	30.82	0.28	78.42
DaG 999	gr5	54.94	0.06	0.51	1.11	11.15	0.41	27.50	3.64	0.02	99.34	26.75	0.23	81.47
DaG 999	gr68	55.34	0.07	0.55	1.11	9.51	0.44	28.32	3.95	0.01	99.30	21.13	0.19	84.15
DaG 999	gr59a	53.13	0.30	1.56	1.35	4.21	0.41	19.62	18.39	0.23	99.20	10.22	0.12	89.25
DaG 999	gr74	56.36	0.12	0.69	1.03	5.07	0.50	31.16	4.51	0.04	99.49	9.93	0.09	91.64
DaG 999	gr92	58.53	0.02	0.09	0.86	4.81	0.37	35.73	0.34	0.00	100.75	12.69	0.08	92.98
DaG 999	gr23**	57.93	0.14	0.41	0.67	1.79	0.49	35.00	2.72	0.05	99.54	3.57	0.03	97.21
DaG 999	gr82a**	55.05	0.30	0.70	0.61	1.11	0.38	22.21	18.94	0.23	99.54	2.93	0.03	97.26
DaG 999	gr85**	58.13	0.14	0.40	0.66	1.79	0.50	35.07	2.70	0.05	99.43	3.50	0.03	97.22
DaG 1000	gr27	54.33	0.08	1.19	1.28	11.79	0.43	26.17	4.33	0.13	99.73	27.22	0.25	79.82
DaG 1000	gr31a	53.15	0.37	1.61	1.43	4.16	0.41	19.08	19.19	0.29	99.67	9.99	0.12	89.11
DaG 1000	gr5	56.13	0.11	0.73	1.03	6.32	0.45	31.98	2.57	0.04	99.36	13.91	0.11	90.01
EET83309	,51 gr25	53.89	0.06	0.77	1.29	13.78	0.41	25.10	4.58	0.09	99.97	33.45	0.31	76.46
EET83309	,50 gr92	53.81	0.04	0.46	1.15	12.67	0.41	27.04	3.52	0.03	99.13	30.86	0.26	79.19
EET83309	,51 gr17	54.52	0.09	1.50	1.30	11.85	0.39	28.13	2.38	0.10	100.25	29.85	0.24	80.89
EET83309	,51 gr16	54.54	0.08	1.49	1.29	11.77	0.39	28.16	2.38	0.09	100.20	29.59	0.23	81.00
EET83309	,51 gr35	55.36	0.06	0.48	1.17	11.31	0.44	27.94	3.45	0.06	100.27	25.42	0.23	81.49
EET83309	,51 gr11	55.75	0.08	0.50	1.16	8.37	0.48	30.02	3.96	0.03	100.35	17.34	0.16	86.47
EET83309	,51 gr18a	53.21	0.24	1.97	1.28	4.32	0.42	20.18	18.35	0.15	100.12	10.05	0.12	89.29
EET83309	,51 gr5a	53.33	0.27	1.72	1.43	4.15	0.40	19.81	18.93	0.28	100.32	10.32	0.12	89.49
EET83309	,50 gr44	56.13	0.10	0.50	1.06	5.65	0.51	31.56	4.30	0.03	99.83	11.00	0.10	90.87
EET87720	,41 gr58	54.63	0.04	0.56	1.25	13.27	0.41	25.97	3.93	0.04	100.10	32.05	0.29	77.73
EET87720	,41 gr26	54.31	0.06	0.77	1.24	12.58	0.41	25.69	4.38	0.04	99.48	30.34	0.27	78.45
EET87720	,41 gr1	54.23	0.05	0.80	1.28	12.10	0.41	25.26	5.12	0.04	99.29	29.13	0.27	78.82
EET87720	,13 gr36	53.71	0.02	0.23	1.14	13.18	0.35	30.58	0.58	0.00	99.80	37.86	0.24	80.57
EET87720	,13 gr08	55.29	0.07	0.67	1.26	9.54	0.45	28.88	3.24	0.05	99.45	20.99	0.19	84.37
EET87720	,13 gr40	55.98	0.01	0.23	1.02	9.73	0.34	31.66	0.55	0.00	99.53	28.61	0.17	85.29
EET87720	,41 gr14	56.76	0.09	0.70	0.84	7.61	0.39	31.72	1.91	0.05	100.05	19.28	0.13	88.14
Nilpena	A gr9	54.71	0.06	0.63	1.15	11.93	0.41	27.94	2.64	0.08	99.56	28.48	0.24	80.68
Nilpena	A gr29	54.88	0.04	0.53	1.30	10.73	0.46	27.94	3.47	0.08	99.44	22.84	0.22	82.27
Nilpena	A gr46	55.36	0.14	0.96	1.15	7.18	0.57	29.07	5.38	0.05	99.84	12.53	0.14	87.83
Nilpena	A gr19a	52.79	0.23	1.87	1.42	4.48	0.41	19.52	18.49	0.23	99.43	10.89	0.13	88.60
North Haig	gr58	54.18	0.04	0.42	1.13	12.71	0.39	26.57	3.06	0.02	98.53	32.02	0.27	78.84
North Haig	gr3	54.75	0.07	0.70	1.13	10.75	0.42	27.26	3.84	0.02	98.94	25.08	0.22	81.88
North Haig	gr16	54.98	0.09	0.85	1.06	9.05	0.42	28.08	4.22	0.07	98.81	21.07	0.18	84.68
North Haig	gr69	55.41	0.11	0.67	0.91	7.66	0.39	31.60	2.37	0.03	99.16	19.35	0.14	88.04
Pyroxenes in ferroan clasts														
EET83309	,50 RC	54.43	0.05	0.18	0.08	19.34	0.40	24.74	0.94	0.03	100.18	48.31	0.44	69.51
EET83309	,51 RC	55.15	0.05	0.16	0.07	19.48	0.39	24.48	0.92	0.02	100.71	49.53	0.45	69.14
Chondritic pyroxenes														
EET83309	,50 gr31	58.72	0.05	0.12	0.03	0.89	0.11	39.37	0.41	0.02	99.70	8.04	0.01	98.75
EET83309	,51 gr20	57.47	0.09	0.52	0.80	4.21	0.50	34.18	2.48	0.03	100.27	8.34	0.07	93.54
EET83309	,51 gr1	59.56	0.00	0.11	0.01	0.36	0.01	39.98	0.18	0.01	100.21	71.01	0.01	99.50
North Haig	gr38a	54.72	0.47	0.46	0.00	0.23	0.01	21.24	21.60	0.26	98.98	32.23	0.01	99.40

Table 3. Ion microprobe oxygen isotope analyses of individual ureilitic clasts[‡].

Sample	n*	mg#	Phase	$\delta^{18}O$ VSMOW ‰	error	$\delta^{17}O$ VSMOW ‰	error	$\Delta^{17}O$ ‰	error
Ureilitic clasts									
EET83309, 51 Gr16	1	81.0	$Wo_{4.7}En_{77.2}$	8.36	0.32	3.69	0.27	-0.66	0.29
EET83309, 51 Gr17	1	80.8	$Wo_{4.7}En_{77.1}$	7.79	0.40	3.67	0.32	-0.38	0.24
EET83309, 51 Gr19	4	79.3	$Fo_{79.3}$	7.94	0.17	3.15	0.14	-0.98	0.14
EET83309, 51 Gr26	1	86.2	$Fo_{86.2}$	6.17	0.32	1.47	0.27	-1.74	0.29
EET83309, 51 Gr35	1	81.5	$Wo_{6.7}En_{76.0}$	7.73	0.40	2.91	0.32	-1.11	0.24
EET83309, 51 Gr20	2	93.5	$Wo_{4.7}En_{89.2}$	5.53	0.28	2.46	0.22	-0.42	0.17
EET87720, 41 Gr1	2	78.8	$Wo_{10.3}En_{70.7}$	8.24	0.18	3.37	0.27	-0.91	0.26
EET87720, 41 Gr14	1	88.1	$Wo_{3.7}En_{84.9}$	6.21	0.45	1.52	0.37	-1.71	0.29
EET87720, 41 Gr20	1	79.0	$Fo_{79.0}$	7.68	0.26	2.72	0.38	-1.27	0.37
EET87720, 41 Gr21	2	82.3	$Fo_{82.3}$	6.95	0.22	2.14	0.31	-1.48	0.25
EET87720, 41 Gr26	1	78.5	$Wo_{8.8}En_{71.6}$	8.53	0.26	3.67	0.38	-0.76	0.37
EET87720, 41 Gr28	1	76.4	$Fo_{76.4}$	8.39	0.32	3.62	0.44	-0.74	0.36
EET87720, 41 Gr29	1	88.5	$Fo_{88.5}$	5.55	0.45	0.88	0.37	-2.01	0.29
EET87720, 41 Gr30	1	77.5	$Fo_{77.5}$	8.27	0.26	3.31	0.38	-0.99	0.37
EET87720, 41 Gr33	2	78.7	$Fo_{78.7}$	7.97	0.26	2.91	0.28	-1.23	0.23
EET87720, 41 Gr37	2	75.0	$Fo_{75.0}$	8.41	0.32	4.12	0.26	-0.25	0.21
EET87720, 41 Gr38[¶]	1	87.6	$Fo_{87.6}$	7.46	0.26	2.70	0.38	-1.18	0.37
EET87720, 41 Gr40	1	79.9	$Fo_{79.9}$	7.74	0.32	2.71	0.44	-1.31	0.36
EET87720, 41 Gr41	1	80.8	$Fo_{80.8}$	7.14	0.45	2.56	0.37	-1.16	0.29
EET87720, 41 Gr44	1	75.4	$Fo_{75.4}$	8.49	0.26	3.80	0.38	-0.62	0.37
EET87720, 41 Gr48	1	77.0	$Fo_{77.0}$	8.28	0.32	3.15	0.44	-1.15	0.36
EET87720, 41 Gr50	1	79.2	$Fo_{79.2}$	7.98	0.45	2.94	0.37	-1.21	0.29
EET87720, 41 Gr58	1	77.7	$Wo_{7.8}En_{71.7}$	8.69	0.45	4.28	0.37	-0.24	0.29
EET87720, 41 Gr60	1	81.7	$Fo_{81.7}$	7.35	0.26	2.51	0.38	-1.31	0.37
EET87720, 41 Gr69	1	79.5	$Fo_{79.5}$	7.69	0.45	2.98	0.37	-1.02	0.29
EET87720, 41 Gr76	1	80.7	$Fo_{80.7}$	7.48	0.32	2.57	0.44	-1.32	0.36
Ferroan Clasts									
EET83309, 51 RC	3	62.1	$Fo_{62.1}$	4.14	0.20	5.50	0.16	3.35	0.16
EET87720, 41 RC	4	63.5	$Fo_{63.5}$	3.28	0.16	1.78	0.20	0.10	0.17
Enstatite meteorite-like									
EET83309, 51 Gr1	1	99.5	$Wo_{0.3}En_{99.2}$	5.64	0.40	2.88	0.32	-0.05	0.24

[‡]Data are corrected for the instrumental mass fractionation by using olivine and pyroxene standards. The quoted errors are 2 standard deviations (2S.D., 95% confidence level) of the repeated analyses of 8-bracketing standard analyses for clasts analyzed only once. For clasts that were analyzed multiple times, the weighted averages and errors were obtained from the individual spot analyses.. *Numbers of repeated spot analyses in the same clasts. [¶]"Hughes cluster" type according to Mn contents.

Table 4. Results of nonparametric Mann-Whitney two-tailed test on olivine mg#s for individual polymict ureilites. "Same" indicates the two populations are statistically the same at the 99% confidence level. Numbers in parentheses are the number of olivine grains in the data set.

	DaG 999	DaG 1000	EET 83309	EET 87720	Nilpena	North Haig
DaG 999 (71)		same	different	same	different	same
DaG 1000 (45)			same	same	different	same
EET 83309 (61)				same	different	same
EET 87720 (63)					different	same
Nilpena (60)						different
North Haig (41)						

EET 83309, 51 Sample length 5mm.

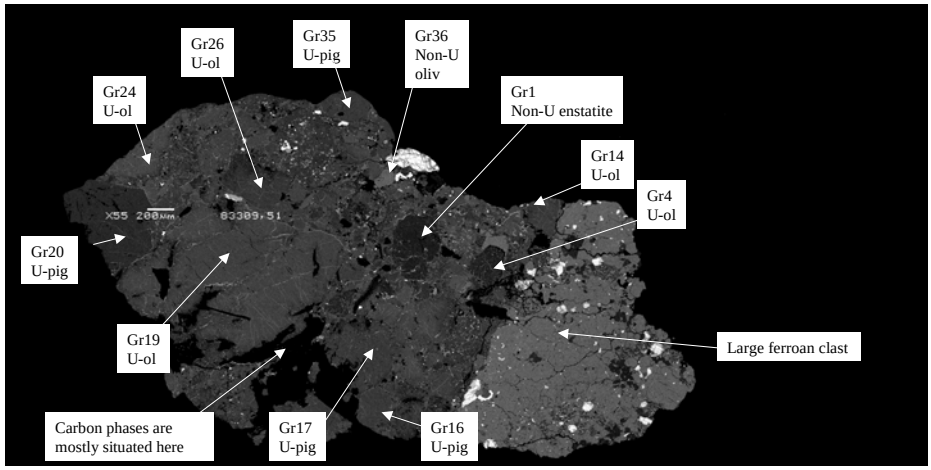

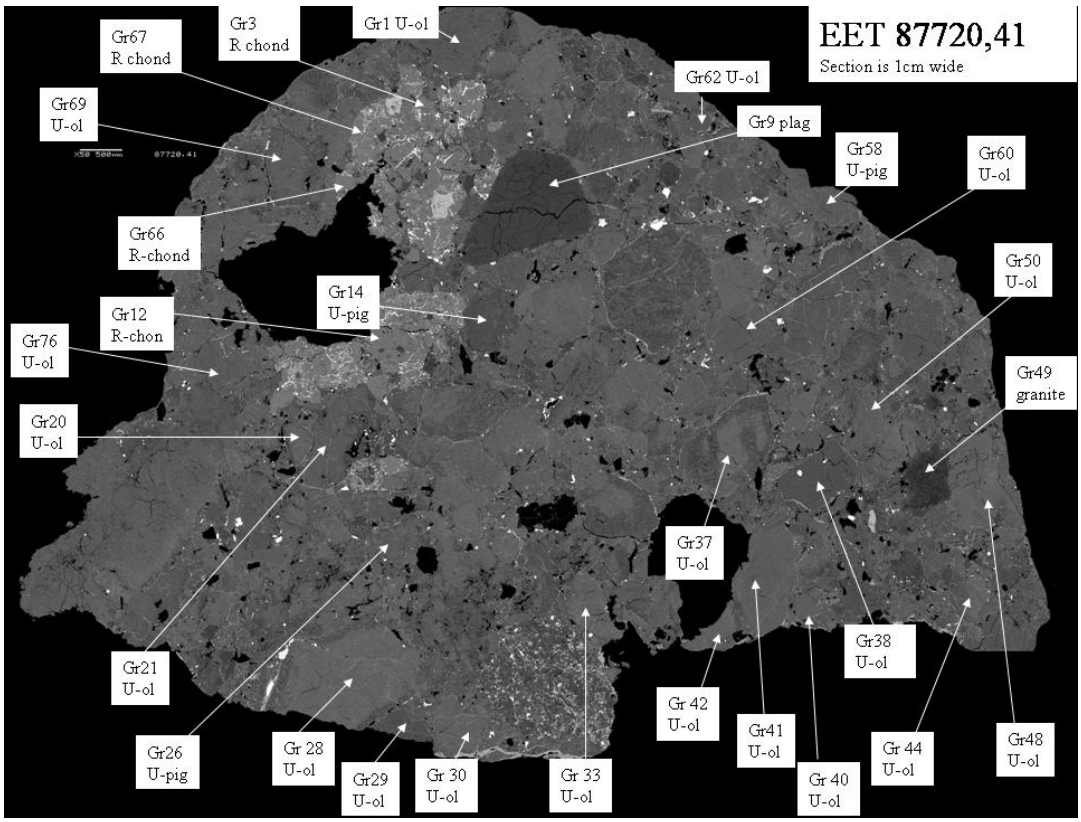

Fig. 1

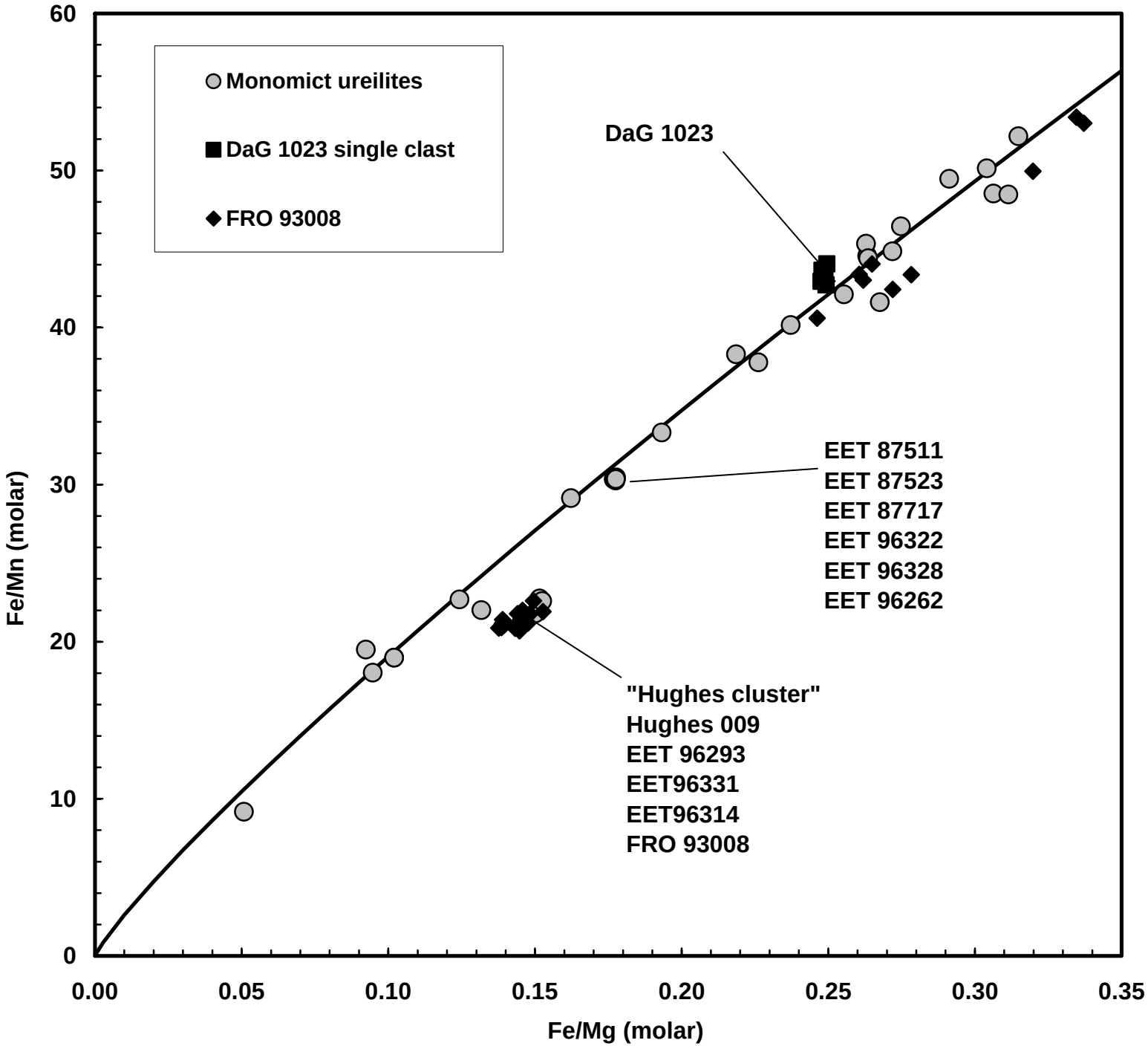
Monomict ureilites
DaG 1023 single clast
FRO 93008
DaG 1023
EET 87511
EET 87523
EET 87717
EET 96322
EET 96328
EET 96262
"Hughes cluster"
Hughes 009
EET 96293
EET96331
EET96314
FRO 93008
Fe/Mn (molar)
Fe/Mg (molar)
0
10
20
30
40
50
60
0.00
0.05
0.10
0.15
0.20
0.25
0.30
0.35

Figure 2

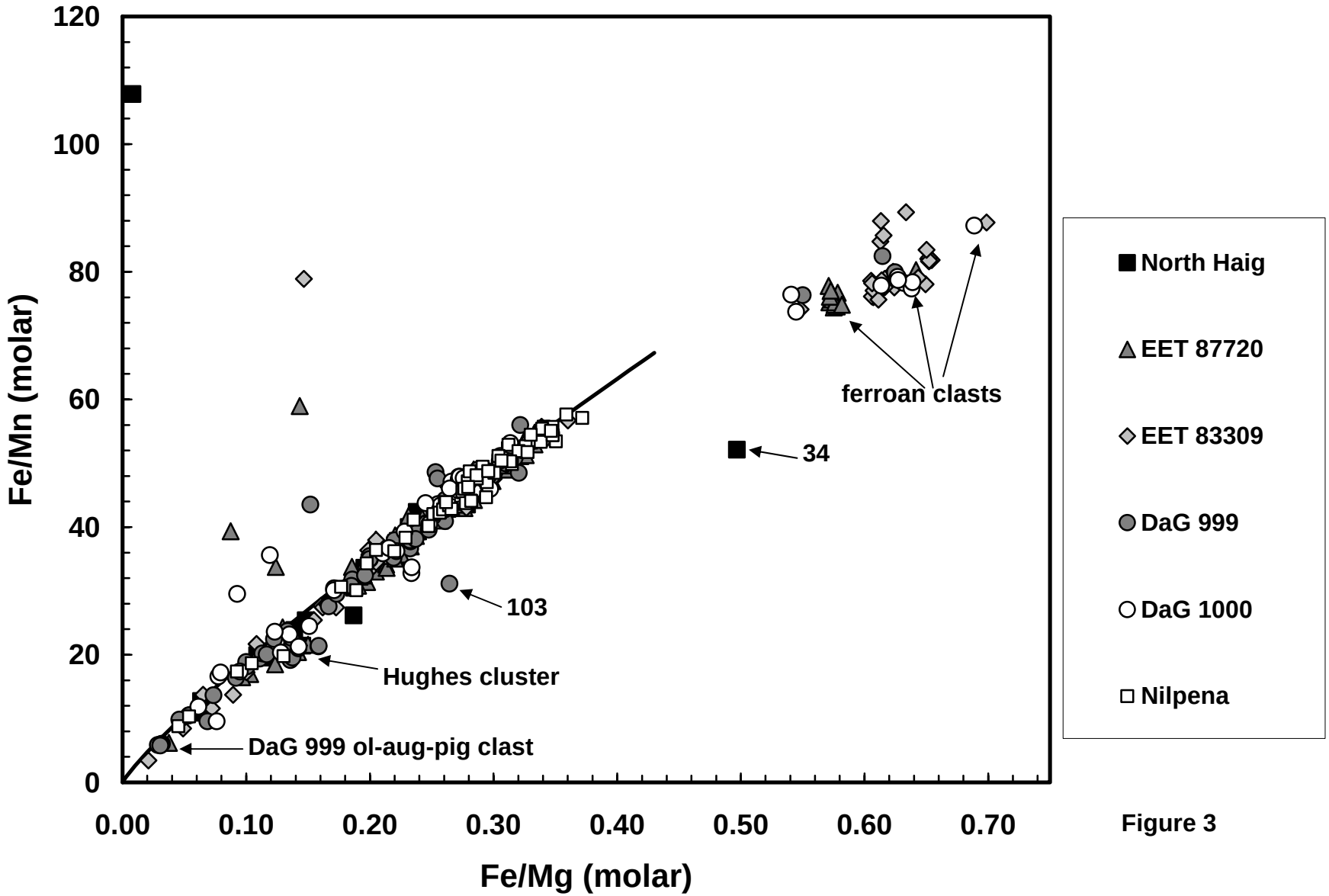
120
100
80
60
40
20
0
Fe/Mn (molar)
0.00
0.10
0.20
0.30
0.40
0.50
0.60
0.70
Fe/Mg (molar)
ferroan clasts
34
103
Hughes cluster
DaG 999 ol-aug-pig clast
North Haig
EET 87720
EET 83309
DaG 999
DaG 1000
Nilpena

Figure 3

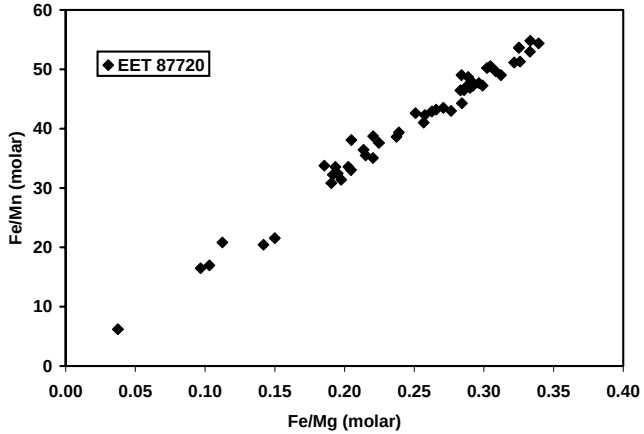
EET 87720
Fe/Mn (molar)
Fe/Mg (molar)

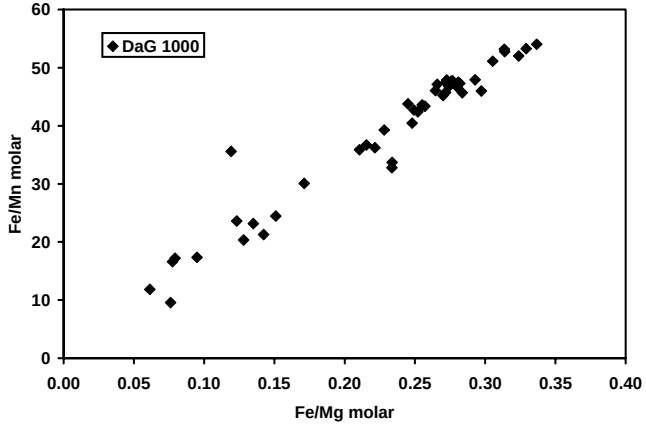
DaG 1000
Fe/Mn molar
Fe/Mg molar

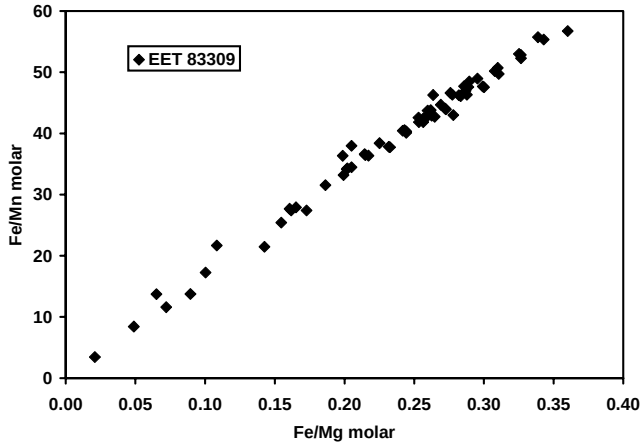
EET 83309
Fe/Mn molar
Fe/Mg molar

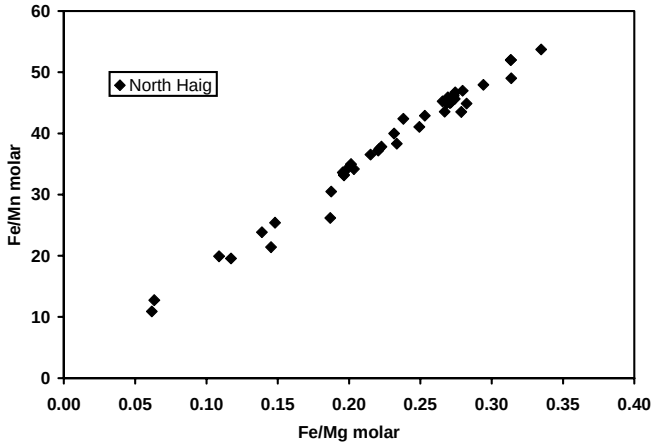
North Haig
Fe/Mn molar
Fe/Mg molar

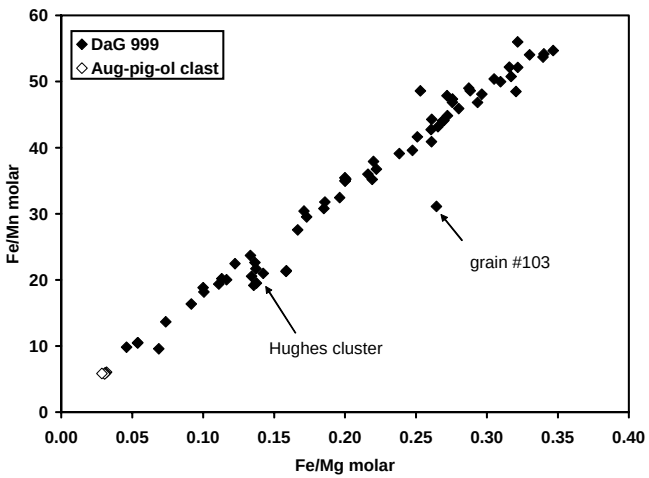
DaG 999
Aug-pig-ol clast
grain #103
Hughes cluster
Fe/Mn molar
Fe/Mg molar

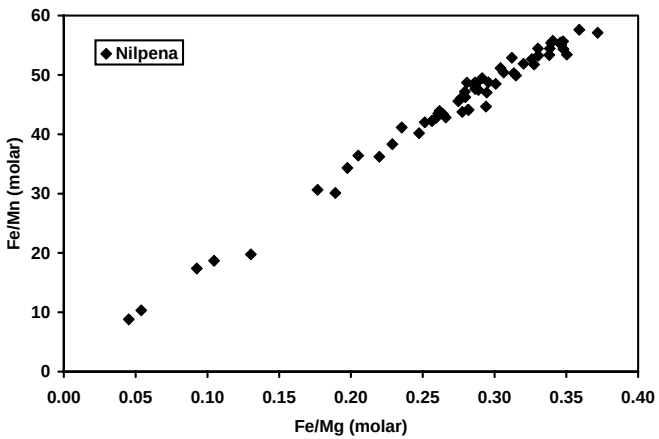
Nilpena
Fe/Mn (molar)
Fe/Mg (molar)

Figure 4

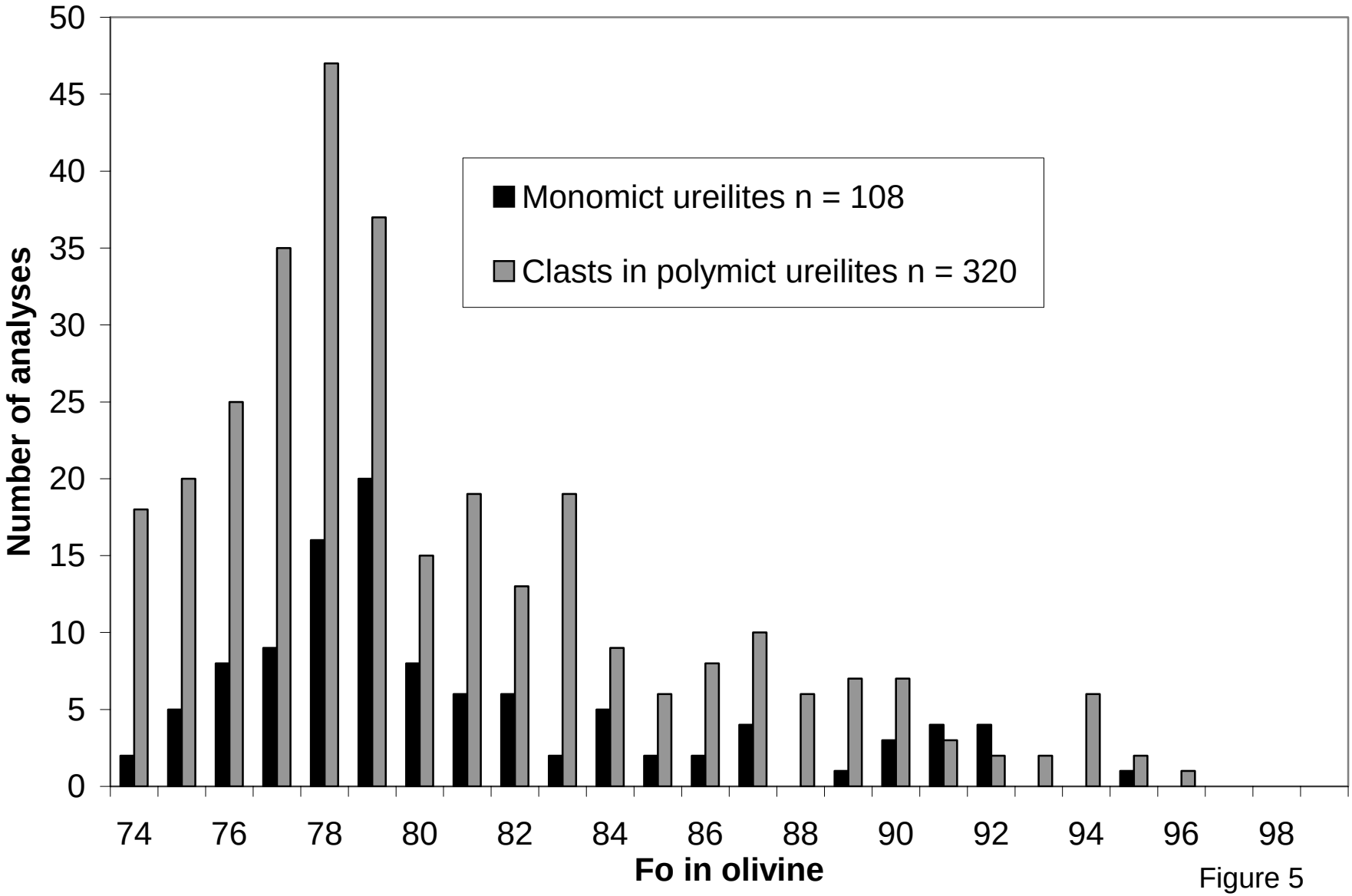
Monomict ureilites n = 108
Clasts in polymict ureilites n = 320
Number of analyses
Fo in olivine
0
5
10
15
20
25
30
35
40
45
50
74
76
78
80
82
84
86
88
90
92
94
96
98

Figure 5

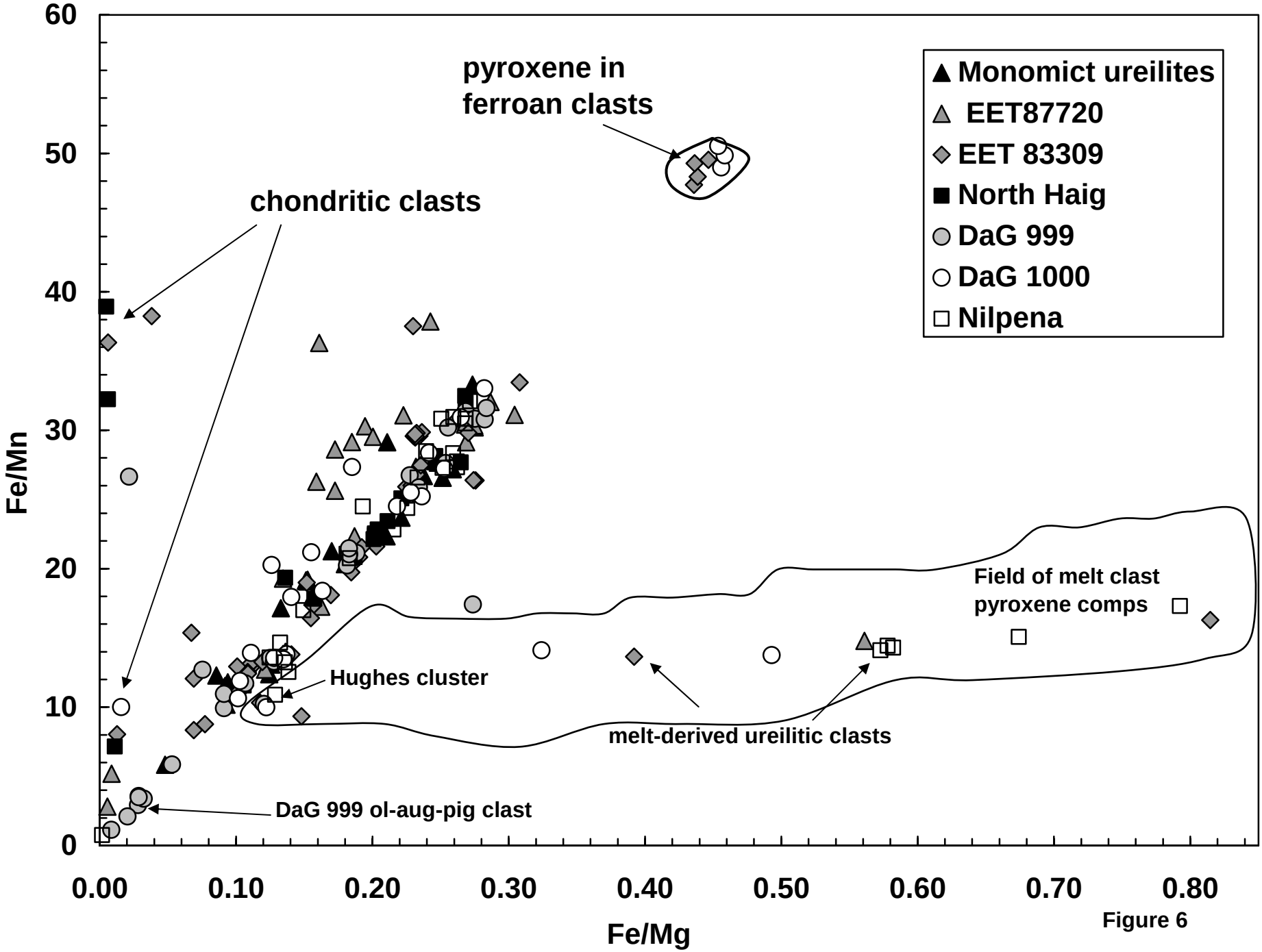
pyroxene in
ferroan clasts
chondritic clasts
Monomict ureilites
EET87720
EET 83309
North Haig
DaG 999
DaG 1000
Nilpena
Field of melt clast
pyroxene comps
Hughes cluster
melt-derived ureilitic clasts
DaG 999 ol-aug-pig clast
Fe/Mn
Fe/Mg
0
10
20
30
40
50
60
0.00
0.10
0.20
0.30
0.40
0.50
0.60
0.70
0.80

Figure 6

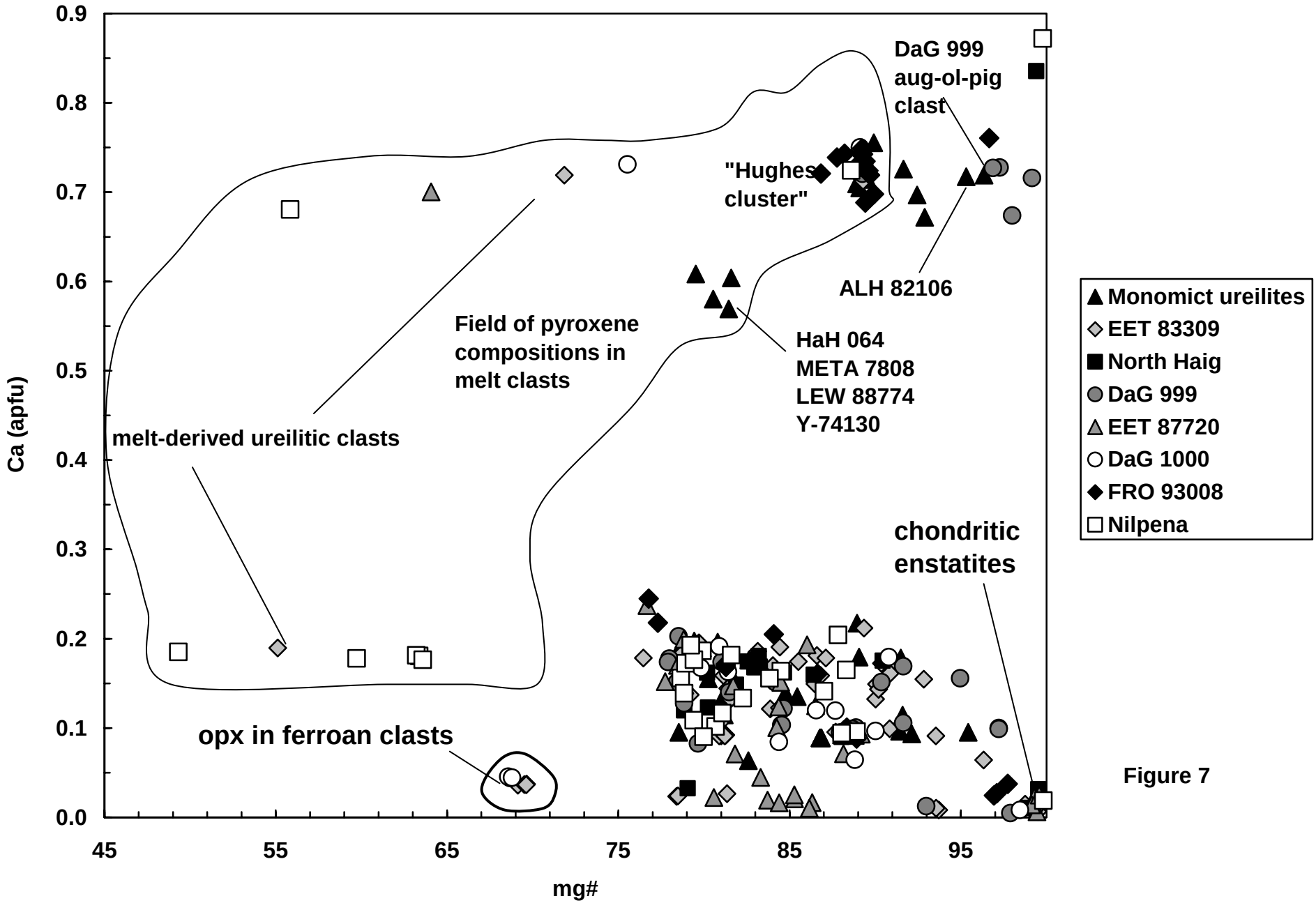
0.9
0.8
0.7
0.6
0.5
0.4
0.3
0.2
0.1
0.0
Ca (apfu)
45
55
65
75
85
95
mg#
DaG 999
aug-ol-pig
clast
"Hughes
cluster"
ALH 82106
Field of pyroxene
compositions in
melt clasts
HaH 064
META 7808
LEW 88774
Y-74130
melt-derived ureilitic clasts
chondritic
enstatites
opx in ferroan clasts
Monomict ureilites
EET 83309
North Haig
DaG 999
EET 87720
DaG 1000
FRO 93008
Nilpena

Figure 7

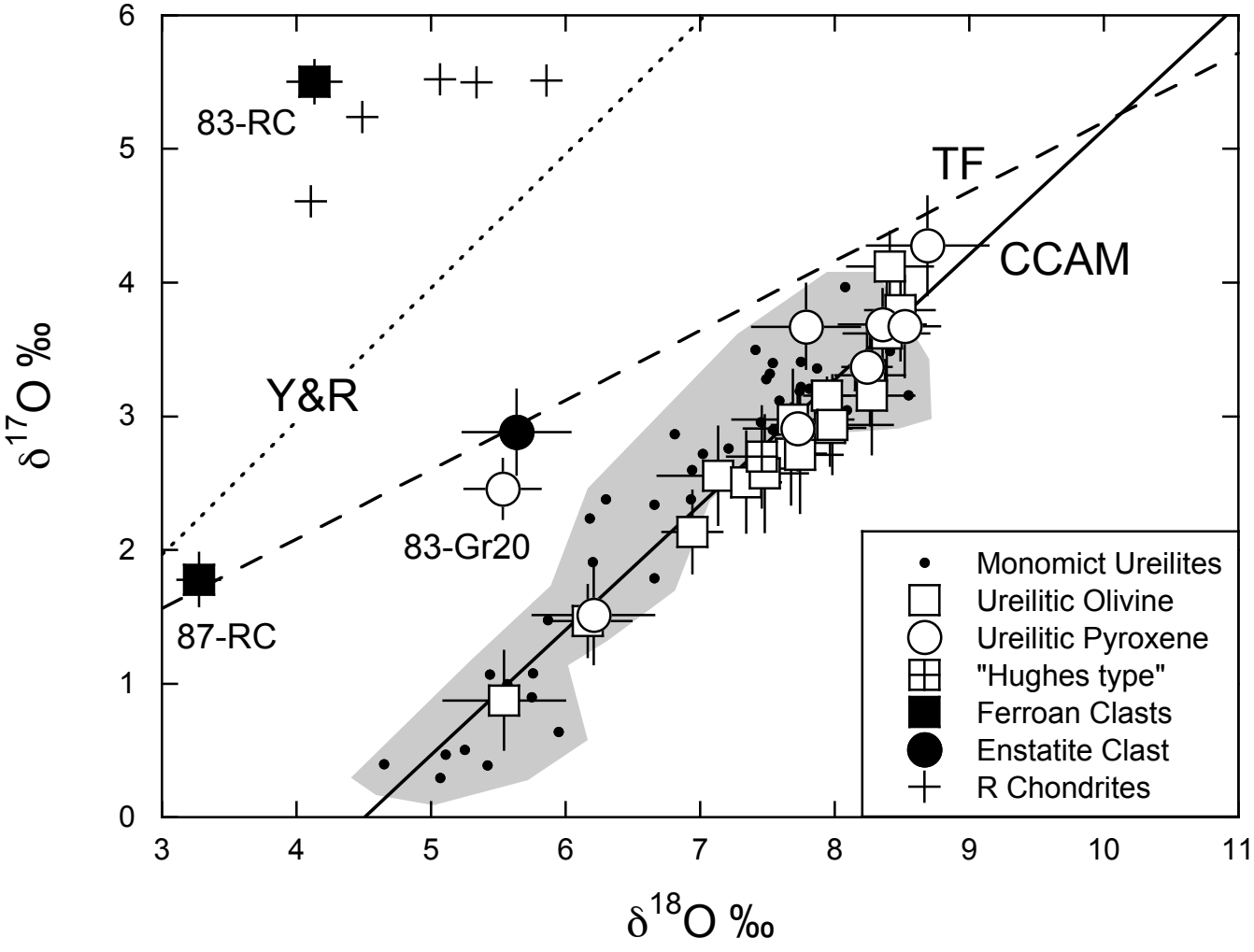
83-RC
TF
CCAM
Y&R
83-Gr20
87-RC
Monomict Ureilites
Ureilitic Olivine
Ureilitic Pyroxene
"Hughes type"
Ferroan Clasts
Enstatite Clast
R Chondrites
δ17O ‰
δ18O ‰
0
1
2
3
4
5
6
3
4
5
6
7
8
9
10
11

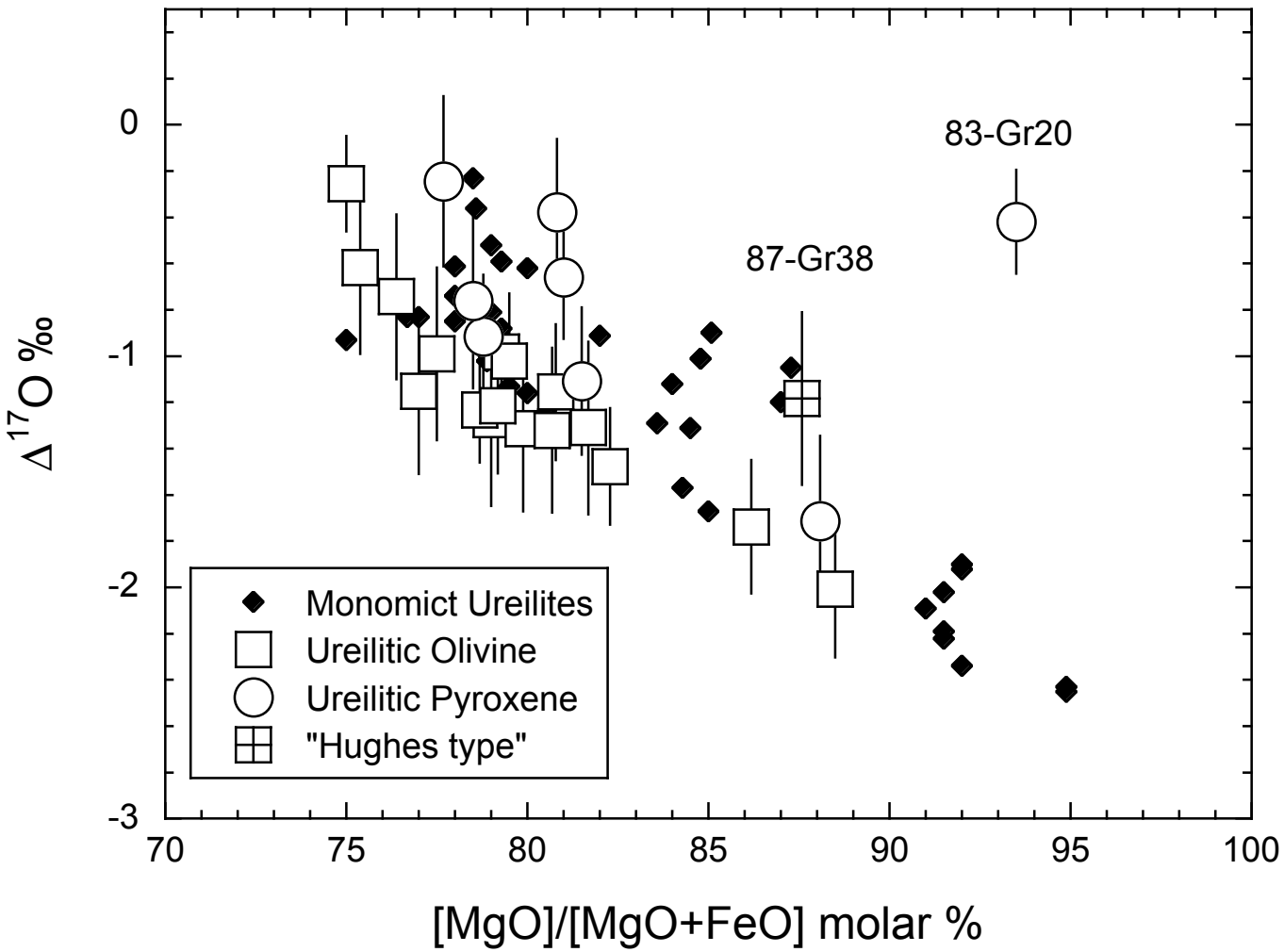
0
-1
-2
-3
70
75
80
85
90
95
100
Δ17O ‰
[MgO]/[MgO+FeO] molar %
83-Gr20
87-Gr38
Monomict Ureilites
Ureilitic Olivine
Ureilitic Pyroxene
"Hughes type"

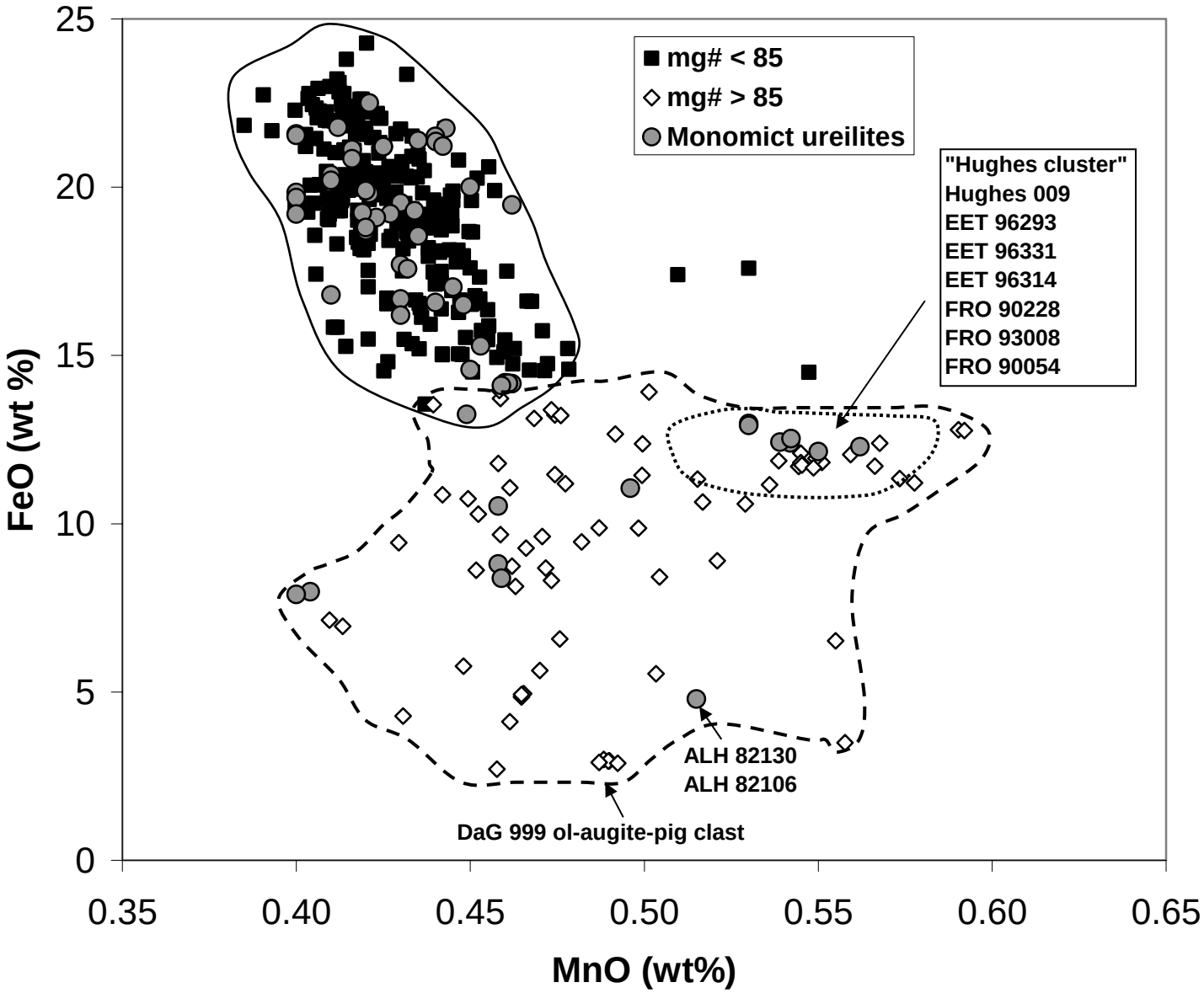
mg# < 85
mg# > 85
Monomict ureilites
"Hughes cluster"
Hughes 009
EET 96293
EET 96331
EET 96314
FRO 90228
FRO 93008
FRO 90054
ALH 82130
ALH 82106
DaG 999 ol-augite-pig clast
FeO (wt %)
MnO (wt%)
0
5
10
15
20
25
0.35
0.40
0.45
0.50
0.55
0.60
0.65

Figure 10